Accepted Manuscript

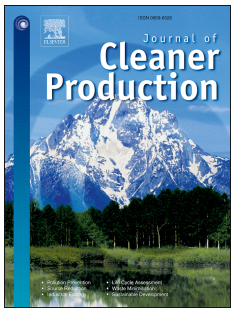

Imparting water repellency in completely decomposed granite with Tung oil

Lin H, Lourenço SDN, Yao T, Zhou Z, Yeung AT, Hallett P, Paton G, Shih K, Hau BCH, Cheuk J

PII: S0959-6526(19)31548-3

DOI: https://doi.org/10.1016/j.jclepro.2019.05.032

Reference: JCLP 16797

To appear in: *Journal of Cleaner Production*

Received Date: 16 June 2018

Revised Date: 24 April 2019

Accepted Date: 3 May 2019

Please cite this article as: H L, SDN Lourenç, T Y, Z Z, AT Y, P H, G P, K S, BCH H, J C, Imparting water repellency in completely decomposed granite with Tung oil, *Journal of Cleaner Production* (2019), doi: https://doi.org/10.1016/j.jclepro.2019.05.032.

Imparting water repellency in completely decomposed granite with Tung oil

Lin H[1], Lourenço SDN[1*], Yao T[1], Zhou Z[1], Yeung AT[1,5], Hallett P[2], Paton G[2], Shih K[1], Hau BCH[3], Cheuk J[4]

[1] Department of Civil Engineering, The University of Hong Kong, Hong Kong SAR

[2] School of Biological Sciences, Aberdeen University, United Kingdom

[3] School of Biological Sciences, The University of Hong Kong, Hong Kong SAR

[4] AECOM Asia, Hong Kong SAR

[5]College of Mining Engineering, Taiyuan University of Technology, Shanxi, People's Republic of China

* Corresponding author

Abstract

Engineered water repellent soils have great potential as construction materials for seepage barriers. By adjusting the water repellency of the soil, an impermeable or semi-permeable seepage barrier can be constructed to suit various engineering applications, such as impervious materials to contain water or semi-permeable materials to allow vegetation growth. Industrial clays, geosynthetics and grouting are proven solutions frequently used for similar applications. To provide a sustainable and low-cost solution to create an engineered water repellent soil, this study explored how Tung oil, a Chinese traditional vegetation oil, affected a Hong Kong completely decomposed granite (CDG). Tung oil has already been used in historical structures and suggested as a self-healing agent for concrete. A natural wettable soil from Hong Kong, CDG, was mixed with Tung oil and heated at different temperatures for different durations. The results reveal that the presence of Tung oil developed severe and persistent water repellency with heating, enhancing water repellency until a critical temperature threshold and heating duration was reached. However, a change to soil physical structure due to aggregation was also observed due to the mixing of the Tung oil with the soil. The newly formed Tung-oil impregnated aggregates were found to be (1) stable when immersed in water, regardless of the temperature and heating duration, (2) and to have increasing tensile strength with aggregate size up to a temperature threshold. Based on these findings, not only can Tung oil induce high and persistent water repellency in a natural soil through simple procedures (by mixing of soil with oil), but also aggregation may offer the opportunity to improve soils for other ground applications including to ameliorate erosion on slopes.

Keywords: Tung-oil, water repellency, completely decomposed granite, soils

1. Introduction

The cost estimates for the construction, maintenance and improvement of ground infrastructure in Hong Kong have doubled in the last decade (Hong Kong 2018-19 Budget, 2018). The need for construction materials that are economic and sustainable is important. The use of synthetic water repellent (or non-wetting, hydrophobic) soils can reduce the carbon footprint in comparison with the use of industrial clays, geosynthetics, or grouting and may have various engineering applications in ground infrastructure. For instance, for completed landfills, an evapotranspiration cover system is required to prevent water percolation in the long run to minimize leachate production. Subedi *et al*. (2013) suggested placing a hydrophobized capillary barrier by using water repellent soils underneath the vegetation layer. Other proposed applications include protection surfaces for horse racing tracks (Bardet *et al*., 2014), waterproof layers in the pavement base of highways (DeBano, 1981) and protection and stabilization of slopes (Zheng *et al*., 2017).

Soil water repellency is a fundamental property, which measures the soil-water interaction, and can be quantified by the contact angle (CA, Ɵ) or water drop penetration time (WDPT). The CA is obtained from Young's equation (Equation 1), derived from the mechanical equilibrium of a water drop on a solid surface with three interfacial tensions, solid-air γ_{sa}, solid-liquid γ_{sl} and liquid-air γ_{la} as:

$$\cos\theta = \frac{\gamma_{sa}-\gamma_{sl}}{\gamma_{la}} \quad (1)$$

A CA > 90° indicates the soil is water repellent (low wettability), while a CA < 90° indicates the soil is wettable (high wettability) (Goebel *et al*., 2011). The WDPT quantifies the persistency of water repellency based on the infiltration rate of a

water drop into the soil (Letey *et al*., 2000). Soil wettability is affected by soil properties such as texture and water content. From tests of water repellent silica sands and glass beads, Saulick *et al.* (2018) found that finer and angular granular materials provide greater CA than coarser and rounded granular materials. In natural water repellent soils, water repellency can also reduce with increasing water content (de Jonge *et al.*, 1999).

Water repellency can be induced in the laboratory by coating soil particles with water repellent substances of a synthetic or natural origin. For natural water repellent soils, it has also been found that the heating temperature, duration and oxygen availability all influence water repellency. Doerr *et al*. (2004) revealed that water repellency increased with temperature up to a threshold, after which the water repellency was eliminated. The threshold depends on the heating duration and soil intrinsic properties such as texture and organic matter (Robichaud & Hungerford, 2000; Savage *et al*., 1972). Oxygen availability is also another factor to take into account. Bryant *et al*. (2005) tested water repellency of soils heated in nitrogen and air, and found that the temperature threshold is higher in a nitrogen atmosphere. As for the durability of the water repellent condition, the lifespan of natural soil water repellency as induced by heating is unknown. However, a monitoring study on a post-wildfire terrain suggests that it can persist for more than five years (Cerdà and Doerr, 2005).

Synthetic coatings have been proposed to induce water repellency in sands. For example, Bardet *et al*. (2014) coated sand particles with water repellent wax coatings. Dimethyldichlorosilane ($(CH_3)_2SiCl_2$, DMDCS), octadecyltrichlorosilane ($CH_3(CH_2)_{17}SiCl_3$) and trimethylchlorosilane ($(CH_3)_3SiCl$) were mixed with sands to obtain water repellent polysiloxanes (Chan & Lourenço, 2016; Ng & Lourenço, 2016). For sands, the results

revealed that 0.001% - 0.005% by mass of these organosilane compounds can result in CAs > 120°. However, for clayey or silty soils, the consumption of silanes is much greater and the water repellency is unstable, thus compromising the cost-effectiveness of the technique. Choi *et al.* (2016) found adding 2.5% by mass of an organosilane compound to a clay induces water repellency. But this water repellency may be short-lived, as observed by Liu (2016) who found that induced water repellency persisted for only one week after the treatment with DMDCS. Therefore, methods to induce stable water repellency in fine soils and which are cost-effective are required. This study proposes a combination of heating and use of a natural water repellent substance, Tung oil, to generate water repellency in fine soils, extending the current range of treatments which are limited to sands or sandy soils.

Tung oil is a traditional Chinese oil obtained from pressing the nut seeds of the Tung Tree (*Vernicia fordii*). It was traditionally used for waterproofing of boat hulls and wooden constructions. Recently, Tung oil has been recognized as a low-cost, clean and durable agent for healing, waterproofing or protection of different materials. For example, Samadzadeh *et al*. (2011) proposed Tung oil as a healing agent to repair scratched wooden surfaces. Chen *et al*. (2017) used Tung oil as a self-healing agent for reinforced concrete. Of interest to this study, Tung oil has been applied to improve the water stability of soil aggregates and durability of earthen construction. Treating natural soils containing 5 -11% of silts and clays with quicklime or Tung oil was found to improve the durability of earthen historical structures (Li & Zhang, 2012). It has also been found that Tung oil could decrease the hydraulic conductivity and wettability of soils (Zhang *et al*., 2016). The longevity of Tung oil under indoor conditions exceeds 25 years (Liu *et al.*, 2015), with one study observing that Tung oil painted on a wooden altar persisted since 1922 (Schönemann *et al.*, 2006).

Tung oil contains approximately 80% of α-eleostearic acid and 20% of a mix of linoleic, palmitic and oleic acids by mass (Zhang et al., 2016). The development of water repellency by Tung oil application to sand depends on the environmental conditions. When subjected to a temperature up to 100°C, it dries and hardens in four stages: (1) inhibition; (2) formation of peroxides; (3) decomposition of peroxides; and (4) polymerization (Wexler, 1964). The formation of a water repellent Tung oil film occurs in stage (4). During heating, fatty acids undergo a melting and re-crystallization process on the surface of sand particles, resulting in more crystalline packed and even coatings, which improves water repellency (Mainwaring et al., 2013). Therefore, heating Tung oil-mixed soils could produce greater water repellency, or the concentration of Tung oil can be decreased to achieve a desired water repellency level.

The addition of Tung oil to a fine-grained soil may not only generate water repellency, but also provide engineering and environmental benefits. Preliminary research conducted within the context of this study has also revealed that: (1) mixing of soil with Tung oil leads to aggregation, i.e. the fines lump to form aggregates; and (2) the aggregates resist wetting without perceptive changes in their structure, e.g. aggregate collapse upon water immersion. These preliminary findings are encouraging, so this study explored the mechanisms controlling aggregation and its durability in a Hong Kong soil. In agricultural sciences, aggregate stability is defined as the ability of a soil aggregate to retain its structure under the action of water or mechanical stress (Dexter, 1988). The former is known as aggregate water stability while the latter is quantified by the aggregate strength. Aggregate stability is an important factor affecting soil properties including the movement and storage of water in soils (i.e. hydraulic characteristics), aeration (i.e. soil air permeability), shear strength (Baumgartl & Horn, 1991; Ekwue, 1990; Fattet *et al*., 2011), erosion and biological activities (Rabot *et al*., 2018; Fattet *et al*.,

2011).

Tung oil also has an economic advantage. With a cost at 7 US$/litre (compared to 106US$/litre for DMDCS), Tung oil presents an economic and sustainable solution for imparting water repellency in soils. As both Tung oil and heating can induce changes to water repellency in soils and aggregate stability, the objective of this study was to determine the combined effects of Tung oil and heating on water repellency and the resulting aggregation behaviour (i.e. aggregate size and stability) of Hong Kong's completely decomposed granite (CDG). The specific objectives were to: (a) study the effects of Tung oil on water repellency of CDG; (b) determine the effect of the heating temperature and duration on water repellency of Tung oil treated CDG; (c) quantify the changes in soil aggregate properties of Tung oil treated CDG followed by heating; and (d) identify the controlling mechanisms on the changes of water repellency and aggregate properties in CDG induced by addition of Tung oil and heating.

2. Methodology

2.1 Materials

2.1.1 Completely Decomposed Granite (CDG)

Approximately 65% of the urban area of Hong Kong is developed on granite. In situ weathering creates decomposed granite (CDG) to form a typical residual soil abundant in Hong Kong. It has been used extensively as fill materials in various applications, such as backfill materials for retaining structures and pavements.

CDG collected from Happy Valley in Hong Kong was selected as the test soil of this study. CDG was originally wettable with a contact angle of 52° (±2.81°).

The results of aggregate size analysis using the dry sieving method (BS 1377-1: 1990) revealed that CDG contains 35% of clays and silts, 49% of sands and 16% of gravel. Other soil properties, such as Atterberg limits and specific gravity, are given in Table 1. Soil organic matter content was determined by loss on ignition (LOI) by heating CDG to 550°C (within 5 hours) (BS 1377 – 3: 1990). Quantitative X-ray diffraction (XRD) analysis was carried out to determine the mineralogy of CDG. Approximately 2 g of soil were pulverized and analysed in an automated powder Philips PW 1710 diffractometer using Cu Kα radiation at 35 kV and 40 mA, between 2 and 70° 2θ at a scan speed of 0.04°2θ/s. The results revealed that the major mineral contents of CDG were quartz and kaolinite (46% and 43%, respectively), accompanied by a small proportion of illite (6%) and gibbsite (5%), as tabulated in Table 1.

2.1.2 Tung oil

The Tung oil used in this study was purchased from Jogel Co., China and contained approximately 80% of α-eleostearic acid, 10% of linoleic acid, 6% of palmitic acid and 4% oleic acid (Zhang *et al*., 2016). It was transparent with an amber color, and a dark residue at the bottom of the bottle. The density was 940 kg/m^3. Only supernatant transparent oil without sediment or other impurities was used for testing.

2.2 Testing procedure

CDG was air-dried in a laboratory environment (~25°C and relative humidity of 60 - 75%), sieved to a particle size of 2 mm followed by mixing and homogenization by hand. The results of preliminary research revealed that 5%

by mass of Tung oil could induce strong or extreme soil water repellency (Doerr *et al*., 2006). Six concentrations by mass of Tung oil (C_{to}) were selected: C_{to}=1%, 2%, 5%, 8%, 10% and 15%. Tung oil was mixed with 1 kg of CDG by hand followed by air drying for 3 days. Preliminary tests found that water repellency induced by Tung oil was stable after 3 days.

Tung oil treated CDG was heated from 50°C to 300°C in 50°C steps in an oven for 0.5, 1 and 3 and 5 hours. After heating, specimens were cooled at room temperature (~25°C) and equilibrated for 7 days (Doerr *et al*., 2005). Triplicate specimens of 10.00±0.01 g at different concentrations of Tung oil heated to different temperatures for different durations were placed in 30 ml ceramic crucibles with a soil thickness of ~5 mm to avoid spatial variation of water repellency caused by temperature gradients (Varela *et al*., 2015).

2.3 Soil wettability measurement

The CA was measured by the sessile drop method (SDM) (Bachmann *et al*., 2000) with a KRÜSS Drop Shape Analyser 25 made in Germany. Firstly, soil particles were sprayed on a double-sided tape on glass slide (27 mm x 77 mm). A 10µL drop of deionized water was placed on the specimen surface from a syringe. The shape of the water drop on the air-water interface was recorded by a camera and the CA was determined by a curve-fitting algorithm (Saulick *et al*., 2017).

The water drop penetration time (WDPT) test was used to assess the persistence of water repellency in CDG. The WDPT test measures the time that water repellency persists on a water repellent soil by placing drops of distilled water on the soil. A water drop volume of 75 µL was selected to be greater than the particle size and voids (Letey *et al*., 2000). The

measurements were conducted in a laboratory environment (22 - 25°C, relative humidity of 60 - 75%) with the time up to 14400 s (Doerr *et al*., 2006).

2.4 Aggregate size analysis

With the addition of Tung oil, the soil particles bonded together to form aggregates which were found to be prone to collapse after heating. To investigate the formation and breakdown of Tung oil treated soil aggregates followed by heating, aggregate size analysis was used by a QICPIC^{TM} Sympatec GmbH dynamic image analyser. Specimens were placed in a vibratory feed to disperse them, followed by free-fall in front of a pulsed light with a high-speed camera.

The Hardin index B_P was used to quantify the changes in aggregate size (Hardin, 1985). B_P was originally applied to quantify the breakage potential of granular materials such as sands. Here, it was adopted to quantify the change in aggregate size in this study. As shown in Figure 1, B_P is equal to the area bounded by 0.074 μm and the ASD curve. A larger B_P corresponds to a larger area, reflecting a shift of the ASD curve towards larger aggregate sizes. In a log-normal distribution, B_P is calculated as follows:

$$B_P = \int_0^1 \log_{10}\left(\frac{D}{d}\right) df \quad (2)$$

where D = the given aggregate size in mm; d = the smallest particle size that can be crushed and assumed to be 0.074 mm (Hardin, 1985); and df = the gradient of the ASD curve.

Scanning electron microscopy (SEM) has been widely used to observe the morphology and surface of soil particles, including water repellent coatings.

Choi *et al*. (2016) observed the surfaces of water repellent clay treated by an organosilane compound while Tang *et al*. (2007) used it for Tung oil treated soils. Here, the SEM was used to observe the aggregation of Tung oil treated CDG in this study by a Hitachi S4800 FEG SEM.

2.5 Aggregate stability assessment

Aggregate water stability and tensile strength were measured on soil aggregates with dimensions 2-3.5 mm to assess the impacts of temperature and duration of heating. Aggregate water stability was measured by immersing six aggregates per test in water (Emerson, 1967). The change of aggregates morphology was recorded by a digital camera with the test ended at either 3,600 s or total breakdown of aggregates. Two parameters were recorded to quantify water stability: (1) the percentage of intact aggregates after 3,600 s (AS_{60}); and (2) the initial breakdown time (T_0) (Li & Zhang, 2012). AS_{60} is the percentage of intact aggregates (not slaking or dispersing) after 3,600 s of water immersion and varies from 0% (all aggregates collapsed) to 100% (all aggregates remain intact). T_0 is the time when the aggregate starts to breakdown and ranges from 0 s to 3,600 s. If all the aggregates remain intact after 3,600 s, they are considered to be water-stable.

Aggregate tensile strength was measured by a single particle compression apparatus built at The University of Hong Kong (Yao, 2019). The test was carried out by placing an aggregate between two stainless steel platens and moving the upper platen at a constant rate of downward displacement of 1.0 mm/h to crush the aggregate. The displacement was recorded by a Linear Variable Differential Transformer (LVDT) with a 2.5 mm linear range and resolution of 0.001 mm. The capacity of the load cell was 100 N with a resolution of 0.1 N. The compression apparatus has been calibrated and

tested preliminarily on a stainless-steel cuboid to ensure the stiffness of the apparatus. The high-resolution of the load cell (0.1N) and LVDT (0.005mm) ensured reliable data (Yao, 2019).

For consistency, air-dried aggregates selected for testing tensile strength were of the same dimensions as those tested for aggregate water stability, *i.e.* 2-3.5 mm. The aggregate tensile strength T_S was calculated by Equation (3):

$$T_S = 0.576 \times \left(\frac{F}{d_a^2}\right) \quad (3)$$

where T_S = aggregate tensile strength (Pa); F = polar force required to fracture the aggregate (N); and d_a = geometric mean diameter of the soil aggregate (m), obtained by Equation (4):

$$d_a = \sqrt[3]{d_x + d_y + d_z} \quad (4)$$

where d_x, d_y, d_z = the longest, intermediate and smallest diameter of each aggregate (m) (Dexter & Kroesbergen, 1985).

2.6 Chemical characterization

To elucidate the mechanisms controlling the wettability changes, Fourier-Transform infrared spectrometry (FTIR) analyses were conducted in untreated CDG specimens (C_{to}=0%), CDG specimens treated with 5% of Tung oil (C_{to}=5%) and CDG specimens treated with 5% Tung oil (C_{to}=5%) followed by heating at different temperatures for different durations. The spectroscopy was performed using a FTIR spectrometer PerkinElmer Spectrum 100 by the KBr pellet method.

To assess the phase change of Tung oil due to elevated temperature and its possible effect on soil water repellency, mass-volume relationship between the soil components were determined. The water repellent soil contains three phases, solids, air and liquids and each phase containing several components as shown in Supplementary Figure 1. The solids (m_s) include soil organic matter and soil minerals and their masses are denoted as m_{om} and m_m, respectively. Liquids (m_l) include soil water and Tung oil, their masses are denoted as m_w and m_{to}, respectively. As a natural soil with organic matter and water content was used, the mass changes of Tung oil only was calculated by deducting the masses of soil organic matter and soil water. To achieve this, testing was conducted in specimens with Tung oil and without Tung oil, i.e. on a control specimen subjected to the same testing procedure. The control specimen was used to obtain the changes of soil organic matter and soil water while the Tung oil treated specimen was to obtain the total mass loss. It is assumed that the soil organic matter and soil water loss is the same for the control and Tung oil treated specimens. The mass change of Tung oil Δm_{to} during heating was obtained by Equation (5):

$$\Delta \mathrm{m_{to}} = \Delta \mathrm{m} - \Delta \mathrm{m_w} - \Delta \mathrm{m_{om}} \quad (5)$$

where Δm = total mass loss (g), Δm_w = soil water mass loss (g); and Δm_{om} = soil organic matter mass loss (g).

3. Effects of Tung oil treatment

3.1 Water repellency

The variations of CA and WDPT of both untreated (concentration of Tung oil - C_{to}=0%) and treated CDG with increasing C_{to} from 1% to 15% are shown in Figure 2. Both CA and WDPT increase with C_{to}, indicating that Tung oil induces water repellency. The CA of untreated wettable CDG was 52° (±2.81°). It was increased to approximately 90° by addition of 1% of Tung oil, and to approximately 124° by increasing C_{to} to 15%. The WDPT of untreated wettable CDG was < 5 s. With addition of 1% of Tung oil, there was no change in the WDPT although the CA was increaseed to ~90°. The increases in WDPT were proportional to C_{to} from 2% to 10% in a logarithmic scale, followed by an increase from approximately 1400 s at C_{to}=10% to approximately 3,600 s at C_{to}=15%.

3.2 Aggregate size, water stability and tensile strength

The SEM images of treated and untreated CDG specimens are shown in Figure 3. Aggregation in the form of bonding of particles was observed with the addition of Tung oil to the soil and after a 3-day drying period. A sand particle (1.5 - 2 mm) covered with fines is shown in Figure 3 (a1). Surface details suggest the presence of clay (plate size ~ 2 µm), supported by XRD that revealed 43% kaolin as shown in Figure 3 (a3). The same material treated with C_{to}=15% is shown in Figure 3 (b1). With increasing magnification, a film (assumed to be Tung oil) covering the whole surface is shown in Figure 3 (b2) and Figure 3 (5b3).

The aggregation process revealed by aggregate size analysis is illustrated in Figure 4. The results of the ASD on untreated (C_{to}=0%) and treated CDG at different concentrations (1% to 15%) are shown in Figure 4(a). In general, the ASD curves shift towards larger aggregate sizes, indicating the aggregate size increases with C_{to}. The changes in B_P and fines content due to the addition of Tung oil are shown in Figure 4(b). It is shown that B_p increases with C_{to}. B_P of untreated CDG (C_{to}=0%) was 2.21. At C_{to} = 1 - 2% there were very limited changes in B_P i.e. 2.27 and 2.19, respectively, followed by an increase to 2.76 at C_{to} = 5%. Fines content decreased continuously from 36% at C_{to} = 0% to 0% at C_{to} = 15%, suggesting particle bonding. The increase in aggregate size of the CDG by Tung oil treatment observed from the ASD curves, as quantified by B_p and fines content, provides evidence for aggregation. The phenomenon is also supported by observations in the SEM images.

Aggregate water stability (AS_{60} and T_0) of treated and untreated CDG was increased by the addition of Tung oil, are tabulated in Table 2. As shown in Figure 5(a), the untreated CDG (C_{to} = 0%) disaggregated in water shortly after immersion. However, the aggregates with small concentrations of Tung oil (C_{to} = 1 - 2%) were stable in water. At C_{to} = 5% and higher, no disaggregation or slaking was observed after 3,600 s, i.e. AS_{60} = 0% (Figure 5(b)).

Aggregate tensile strength measurements revealed two patterns of stress-strain curves (Figure 6(a)). Aggregates can be either ductile or brittle (Dexter, 1985). Pattern 1 suggests a softer aggregate (possibly with more fines) with the aggregate flattening during the compression. In pattern 2 a sharp drop in stress occurs, suggesting a stiffer aggregate (possibly with fewer fines) failing by brittle fracture. The aggregate tensile strength as shown in Figure 6(b) is determined from the peak strength. Clean sand grains are stiff and the peak strength cannot be measured due to the limited capacity of the load cell.

Aggregate tensile strength T_S increased with Tung oil concentration C_{to} (Figure 6(b)). For the untreated CDG (C_{to} = 0%), T_S = 51.9 kPa which remained approximately constant from 1% to 2%, i.e.65.3 kPa and 52.5 kPa at 1% and 2%, respectively. These values are comparable to those obtained in other studies, e.g. 63 - 89 kPa in Munkholm *et al*. (2016); 59 - 175 kPa in Stumpf *et al*. (2018). For C_{to} = 5%, Tung oil enhances the aggregate tensile strength of CDG from ~50kPa to 238.3 kPa. At higher concentrations of Tung oil, the T_S increases to 925.2 kPa at C_{to} = 10% and remained stable at C_{to} = 15%, i.e. 925.6 kPa. The tensile strength standard deviation (30~40%) was due to the variation of the aggregate size, shape and composition, which was comparable to reported values by similar compression apparatus and testing procedures (25~40%) (e.g. Obaluma et al., 2019; Munkholm et al., 2016). These results reveal that the addition of Tung oil not only improves aggregate water stability, but also increases aggregate tensile strength.

4. Effects of heating

4.1 Water repellency

The effects of heating (i.e. temperature from 50°C to 300°C and duration from 0.5 to 5 hours) on the CAs at increasing C_{to} (0% to 15%) are shown in Figure 7. At heating durations of 0.5 to 3 hours, CA curves shifts upwards with increases in C_{to} as shown in Figures 7(a), 7(b) and 7(c), indicating that heating enhanced water repellency. At 50 - 100°C, CAs were around 100° at C_{to} = 1%, followed by an increase to approximately 120° at C_{to} = 10%. However, a longer heating duration of 5 hours increased soil water repellency up to a threshold temperature. As shown in Figure 7(d), the CAs of treated CDG reach the maximum after heating at 150°C for 5 hours to approximately 115 - 120° at

C_{to}= 1 - 2% and 120 - 125° at higher C_{to} of 5 - 15%. This was followed by a decrease of CAs from heating temperature of 200-300°C. At low concentrations C_{to} = 1 - 2%, the CAs reduce to 80 - 100° at heating temperatures of 200 - 250°C and approximately 20° at 300°C, respectively. At higher concentrations of C_{to} = 5 - 15%, CAs also reveal a reduction but remain >90° after heating in the range of 200 - 300°C, indicating that soils were still water repellent.

The effects of heating on the persistency of water repellency, i.e. WDPT, are shown in Figure 8. At heating durations of 0.5 to 3 hours, the C_{to} versus WDPT curves shift upwards as shown in Figures 8(a), 8(b) and 8(c), indicating that heating enhances soil water repellency. At the longer heating duration of 5 hours, WDPT increased with temperature from 50 to 250°C, followed by a reduction at 300°C as shown in Figure 8(d). The variation of WDPTs

was consistent with the variation of CAs.

A linear correlation between the soil organic matter and the logarithmic WDPT value has been demonstrated in soil science for natural water repellent soils (McKissock *et al*., 1998; Mataix-Solera & Doerr, 2004; Täumer *et al*., 2005). In this study, this correlation is applied to quantify the effects of Tung oil and heating on soil water repellency. A regression line was fit through each of the WDPT/Tung oil concentration curves to determine their gradients, E_A using Equation (6):

$$E_A = \frac{\log(\mathrm{WDPT}) - B}{C_{to}} \quad (6)$$

where E_A = gradient of the regression line, C_{to} = Tung oil concentration by mass; and B = a fitting coefficient. A larger E_A indicates Tung oil is more effective at inducing water repellency. The results for E_A are tabulated in Table

3. The gradient increases with the heating temperature as shown in Figure 9. At 0.5-hour heating duration, the gradient was similar in a range of 50 - 150°C. At the heating temperature of 200°C, the gradient increased to approximately 0.7 and remained stable at higher temperatures of 250 - 300°C. At 1 - 3-hour heating duration, the gradient increased steadily from approximately 0.26 at 50°C to approximately 0.9 at 300°C. The curves for 1-hour and 3-hour heating durations overlap each other, suggesting that heating causes a similar water repellency. For a duration of 5 hours, the gradient was similar in the range 50 - 200°C as those in 1 - 3-hour heating durations. However, at high temperatures of 250 - 300°C, the gradient decreased to 0.41 - 0.47.

4.2 Aggregate size, water stability and tensile strength

The effects of heating on the Hardin index (B_P) are depicted in Figure 10. The results reveal that B_P was stable at temperatures from 50 - 100°C and decreased at higher temperatures of 150 - 300°C. As for Tung oil concentration, B_P at C_{to}= 0 - 2% was 2.0 - 2.4 and not influenced by heating. At higher Tung oil concentrations of 5 - 15%, B_P decreased from 2.6 - 2.7 at 50 - 100°C to 2.2 - 2.3 at 150 - 300°C. However, the heating duration did not influence B_P.

The results of aggregate water stability (AS_{60} and T_0) of CDG with C_{to} = 0 - 15% under different heating conditions are tabulated in Table 2, indicating that the water stability was not affected by heating.

The aggregate tensile strengths with C_{to} = 15% under different heating conditions are compared in Figure 11. The results reveal that the aggregate tensile strength was stable in a range of 50 - 150°C. However, at the high temperature of 300°C, T_S can be influenced by heating duration. For unheated

CDG, T_S = 925.6 kPa. Heating at 50°C did not change T_S significantly, i.e. 955.6kPa for 0.5 hour and 909.8 kPa for 5 hours, respectively. When heated at 150°C, T_S increased slightly to 967.2 kPa for 0.5 hour and to 972.2 for 5 hours. When heated at 300°C, T_S increased to 1133.3 kPa for 0.5 hours but reduced to 925.6 kPa for 5 hours.

4.3 Tung oil loss

To ascertain the influence of the Tung oil loss with heating and time, and its possible effects to wettability, the average mass change of Tung oil (ΔTO) in percentage at six different initial Tung oil concentrations was determined by:

$$\Delta\mathrm{TO} = (\sum \frac{\Delta m_{to}}{m_0 \times C_{to}} \times 100\%)/6 \quad (7)$$

where ΔTO = average mass change of Tung oil at six different initial Tung oil concentrations from 1% to 15%; Δm_{to} = mass change of Tung oil for each specimen; C_{to} = the initial Tung oil concentration of the specimen; and m_0 = mass of CDG equal to 10.00g. It is assumed that all treated CDG specimens were subjected to the same SOM and soil water change as untreated CDG.

As shown in Figure 12, ΔTO increased with heating temperature and duration. In a range of 50 - 150°C, the average mass loss of Tung oil was smaller than 5% - 10%. In this range, the heating duration had no influence on the change of Tung oil mass. While at higher temperatures of 200 - 300°C, the average mass loss was larger and increased with heating duration, i.e. 2.5% - 14% for 0.5-hour heating duration, 6% - 24% for 1-hour heating duration and 7% - 28% for 3 - 5-hour durations.

The decrease of ΔTO in the range 50 - 150°C could result from the evaporation of VOCs in Tung oil. At heating temperatures higher than 150°C, the Tung oil may be subjected to oxidation, evaporation and chemical changes.

4.4 FTIR Results

The spectrum of the untreated CDG (the mineral content) is shown in Figure 13(a). Absorption in the 3750–3570 cm^{-1} region is representative of the hydroxyl (O-H) stretching vibrations of kaolinite (McKissock *et al*., 2003; Saikia & Parthasarathy, 2010). The bands at 1100 cm^{-1}, 1035 cm^{-1} and 913 cm^{-1} are attributed to symmetric Si-O out-of-plane stretching, in-plane Si-O stretching and O-H deformation of kaolinite, respectively (Linker *et al*., 2005). The double peaks of 797 and 780 cm^{-1} are the fingerprint regions of quartz. However, , only the absorption of 797 cm^{-1} can be identified in the spectrum. Hematite is identified by two peaks at 540 cm^{-1} and 471 cm^{-1} (Salama *et al*., 2015).

The spectrum of Tung oil shown in Figure 13(b) reveals water repellent functional groups. The presence of 3012 cm^{-1} is representative of the C-H stretching vibrations of the alkenyl group. The peaks at 2926 cm^{-1} and 2850 cm^{-1} are the symmetric and asymmetric C-H stretching vibration of the methyl group (Schönemann & Edwards, 2011), which were mostly produced by α-eleostearic acid (representing ~80% of the Tung oil). The most intense peak observed in the spectrum was 1745 cm^{-1}, confirming the presence of hydrogen-bonded carboxyl groups (Schönemann & Edwards, 2011). The absorptions of 992 cm^{-1} and 965 cm^{-1} are ascribed to the C=C stretching of the conjugate alkenyl groups of α-eleostearic acid. The peak at 728 cm^{-1} also corresponds to C-H bending vibration of the cis-configuration of the alkenyl group.

An FTIR analysis was conducted in Tung oil treated CDG in both unheated and heated states (150 and 300°C for 5 hours) as shown in Figure 13(c). The results reveal a change of the functional groups in the Tung oil due to the exposure to elevated temperature while no change of the mineral content was observed, as the fingerprint regions of kaolinite and quartz remain the same. The treated CDG reveals adsorption at 1623 cm^{-1}, representative of the C-O stretching vibration of COO- (Celi *et al*., 1997) after heating. The band at 1745 cm^{-1} vanishes after heating to a temperature from 150 to 300°C, indicating the reaction of carboxyl groups (COOH) in Tung oil and metal oxide groups in CDG after heating. Change of spectra in the 3400 cm^{-1} band is often due to the contamination of the specimen by water during the FTIR analysis (Kaiser and Ellerbrock, 2005). The results of FTIR analysis confirm that Tong oil partly reacts with CDG after heating at 150°C for 5 hours and Tong oil totally reacts with CDG and forms a coordination bond with CDG after heating at 300°C for 5 hours.

5. Discussion

5.1 Water repellency development

Water repellency of CDG was induced by the addition of Tung oil as shown in Figures 2. As described in Section 2, over the 3-day drying period, Tung oil would have hardened in four stages (Wexler, 1964) with high and persistent water repellency developed in the last stage (polymerization).

Heating can increase or decrease soil water repellency depending on the heating temperature and duration. The enhancement and reduction of water repellency can be explained by these mechanisms:

(1) Melting of organic compounds: Savage *et al*. (1972) suggested that heating could melt the solid organic compounds, resulting in a continuous coating on sand particles (Laskowski & Kitchener, 1969; Ma'shum *et al*., 1988) which enlarge the water repellent regions and increase water repellency.

(2) Isomerization of cis-unsaturated to trans-unsaturated acids: the bent hydrocarbon chains in the α-eleostearic acids of Tung oil can isomerize to all-trans octadecatrienoic acids, i.e. β-eleostearic acids, which straighten during heating as shown in Figure 14(a). Mainwaring *et al*. (2013) suggested that the straight hydrocarbon chains pack more efficiently, in comparison with the bent chains, leading to enhanced water repellency.

(3) Orientation change of molecules on soil particle surfaces: FTIR anslysis detected a change from COOH to COO^- in Tung oil and reaction with metal oxide groups in CDG during heating, which may suggest a change in the water repellency magnitude. To illustrate mechanisms (2) and (3), the isomerization of cis-trans fatty acid molecules (bent hydrocarbon chains to straight hydrocarbon chains) and the change of headgroups (COOH to COO^-) is shown in Figure 14(a); and the interaction between COO^- and the particle surfaces is shown in Figure 14(b), with the molecules arrayed at the soil surface providing water repellency (Doerr *et al*., 2000; Graber *et al*., 2009).

(4) Combustion or evaporation of Tung oil: the decrease in water repellency under extreme heating conditions, i.e.250 - 300°C for 5 hours, can be due to the oxidation of Tung oil, which occurs at 275 - 350°C with the oxidation process lasting for more than 1 hour (Fuller, 1931), or the elimination of the water repellent C-H groups, i.e. 2969 and 2850 cm^{-1} in the FTIR spectrum shown in Figure 13(c). Moreover, the mass analysis

presented in Section 6.4 indicates that under these extreme heating conditions, the average loss of Tung oil was greater than 25% as shown in Figure 12 which may reduce or discontinue the oil films exposing the wettable mineral surfaces.

5.2 Aggregation

Both soil aggregate water stability and tensile strength were enhanced by the addition of Tung oil. The improved aggregate water stability can be explained by the presence of water repellency, which blocks water penetration into the pores, while the increased aggregate tensile strength can be attributed to the Tung oil hardening and bonding. Kořenková & Matúš (2015) revealed a positive correlation between soil water stability and the severity of water repellency, while Goebel *et al*. (2005) revealed that water repellent conditions on aggregate surfaces could slow the mineralization of soil organic matter and enhance the water stability of aggregates.

Heating had no influence on aggregate water stability. The extreme water repellency may have inhibited the water penetration and slaking. Even under extreme heating conditions, i.e. 250 - 300°C for 5 hours, where a reduction in water repellency was likely, the CAs were still greater than 90° and the WDPTs were still longer than 14400 s for a Tung oil concentration higher than 5%.

For the aggregate tensile strength, heating at 50°C induced limited effect on the T_S while at 150°C the strength increased slightly with duration as shown in Figure 11. These slight variations of T_S at low temperatures of 50 - 150°C may be attributed to the varying ambient temperature (~25°C) and relative humidity (60 - 75%). After heating at 300°C, the increase in T_S after a short heating duration of 0.5 hour could result from the thermal polymerization of Tung oil,

while the decrease in T_S after a long heating duration of 5 hours might be due to the Tung oil loss as shown in Figure 12.

6. Conclusions

This study proposes a novel method to induce water repellency in wettable CDG by mixing with Tung oil followed by heating. By analyzing the influence of Tung oil concentration, and heating temperature and duration, on soil water repellency, soil aggregate size, aggregate water stability and aggregate tensile strength, the following conclusions have been drawn:

(1) Tung oil can develop high and persistent water repellency in natural wettable CDG. Using a relative high concentration of Tung oil, both severity and persistence of water repellency as measured by CA and WDPT were improved, as a result of the formation of water repellent oil films covering soil particle surfaces.

(2) Heating can enhance water repellency up to a temperature threshold and depending on the heating duration. The positive effect of heating towards water repellency could result from (a) melting of organic compounds; (b) isomerization of cis-to-trans unsaturated acids; and (c) orientation change of fatty acid molecules; while diminishing water repellency with heating results from Tung oil loss.

(3) The addition of Tung oil to CDG results in soil aggregation caused by particle bonding, while heating at high temperatures of 150 - 300°C afterwards results in the breakdown of soil aggregates.

(4) The addition of Tung oil enhances aggregate water stability and increases aggregate tensile strength. Improved aggregate water stability could be a result of water repellency which prevents water penetration. The increase in aggregate tensile strength could be attributed to the Tung oil bonding among soil particles and subsequent hardening of Tung oil.

(5) Heating shows no influence on aggregate water stability, as the aggregates are still water repellent after heating, preventing water penetration and inhibiting their slaking. The aggregate tensile strength depends on the heating temperature its duration. Up to 150°C, it remained stable. At 300°C, T_S increased after 0.5-hour heating, possibly due to thermal polymerization but decreased after 5.0-hour heating possibly due to Tung oil loss.

(6) With a cost at 7 US$/liter (comparing to 106 US$/liter for DMDCS), Tung oil is a cost-effective solution to induce water repellency in soils. If unheated, its negligible CO_2 consumption will contribute towards the sustainability of engineering projects. Tung-oil treated soils will find applications in barriers to control infiltration due to their high and stable water repellency. Aggregation may also translate into benefits in erosion control. Benefits to other applications also include increase in shear strength due to a higher cohesion (Fattet *et al*., 2011). While its durability has not been investigated, its water immersion stability and increase in aggregate tensile strength suggest that it may be environmentally stable and long-lasting. Shogren *et al*. (2004) evaluated the degradation of selected vegetation oils. Their results revealed that only approximately 10% of Tung oil degraded after a 30-day accelerated aging test, suggesting the mineralization of Tung oil was slower than those of other vegetation oils such as soy and linseed oil.

Acknowledgements

This research was supported by the General Research Fund, Research Grants Council of Hong Kong under Grant No. 17221016. P. Hallett receives support from the UK Engineering and Physical Sciences Research Council (EP/M019713). Mr. Anthony Oldroyd of the School of Earth and Ocean

Sciences of Cardiff University, U.K. conducted the XRD analysis. Technical support for other testing was provided by Mr. N.C. Poon of the Department of Civil Engineering of The University of Hong Kong. The support is gratefully acknowledged.

References

Bachmann, J., Horton, R., Van Der Ploeg, R. R., & Woche, S. (2000). Modified sessile drop method for assessing initial soil-water contact angle of sandy soil. Soil *Science Society of America Journal, 64(2),* 564-567. doi:10.2136/sssaj2000.642564x

Bardet, J.-P., Jesmani, M., & Jabbari, N. (2014). Permeability and compressibility of wax-coated sands. *Géotechnique, 64(5),* 341-350. doi:10.1680/geot.13.P.118

Baumgartl, Th., & Horn, R. (1991). Effect of aggregate stability on soil compaction. *Soil and Tillage Research, 19(2-3),* 203-213. doi:10.1016/0167-1987(91)90088-F

Bryant, R., Doerr, S. H., & Helbig, M. (2005). Effect of oxygen deprivation on soil hydrophobicity during heating. *International Journal of Wildland Fire, 14(4),* 449-455. doi:10.1071/WF05035

British Standards Institution. (1990a). Methods of test for soils for civil engineering purposes. General requirements and sample preparation. British Standard 1377-1:1990, London.

British Standards Institution. (1990b). Methods of test for soils for civil engineering purposes. Chemical and electro-chemical tests. British Standard 1377-3:1990, London.

Capriel, P., Beck, T., Borchert, H., Gronholz, J., & Zachmann, G. (1995). Hydrophobicity of the organic matter in arable soils. *Soil Biology and Biochemistry, 28(11),* 1453-1458. doi:10.1016/0038-0717(95)00068-P

Celi, L., Schnitzer, M., & Negre, M. (1997). Analysis of carboxyl groups in soil humic acids by wet chemical method, Fourier-Transform infrared spectrometry and solution-state carbon-13 nuclear magnetic resonance: a comparative study. *Soil Science, 162(3),* 189-197. doi:10.1097/00010694-199703000-00004

Cerdà A., Doerr S.H. (2005). The influence of vegetation recovery on soil hydrology and erodibility following fire: an eleven year investigation. *International Journal of Wildland Fire 14(4)*, 423–437

Chan, S.H., & Lourenço, S.D.N. (2016). Comparison of three silane compounds to impart water repellency in an industrial sand. *Géotechnique Letters, 6(4),* 1-4. doi:10.1680/jgele.16.00097

Chen, Y.X., Xia, C., Shepard, Z., Smith, N., Rice, N., Peterson, A.M., & Sakulich, A. (2017). Self-Healing Coatings for Steel-Reinforced Concrete. *ACS Sustainable Chemistry & Engineering, 5(5),* 3955-3962. doi:10.1021/acssuschemeng.6b03142

Choi, Y., Choo, H., Yun, T., Lee, C., & Lee, W. (2016). Engineering characteristics of chemically treated water-repellent kaolin. *Materials, 9(12),* 978. doi:10.3390/ma9120978

DeBano, L.F. (1981). *Water Repellent Soils: A State-of-the-Art.* Washington, D.C., USDA Forest Service General Technical Report PS W-46

DeBano, L.F. (2000). The role of fire and soil heating on water repellency in wildland environments: A review. *Journal of Hydrology, 231-232,* 195-206. doi:10.1016/S0022-1694(00)00194-3

Dekker, L.W., Ritsema, C.J., Oostindie, K., Moore, D., & Wesseling, J.G. (2009). Methods for determining soil water repellency on field-moist samples. *Water Resources Research, 45(4),* W00D33. doi:10.1029/2008WR007070

Dexter, A.R. (1988). Advances in characterization of soil structure. *Soil and*

Tillage Research, 11(3-4), 199-238. doi:10.1016/0167-1987(88)90002-5

Dexter, A.R., & Kroesbergen, B. (1985). Methodology for determination of tensile strength of soil aggregates. *Journal of Agricultural Engineering Research, 31(2),* 139-147. doi:10.1016/0021-8634(85)90066-6

Doerr, S.H., Blake, W.H., Shakesby, R.A., Stagnitti, F., Vuurens, S.H., Humphreys, G.S., & Wallbrink, P. (2004). Heating effects on water repellency in Australian eucalypt forest soils and their value in estimating wildfire soil temperatures. *International Journal of Wildland Fire, 13(2),* 157-163. doi: 10.1071/wf03051

Doerr, S.H., Douglas, P., Evans, R.C., Morley, C.P., Mullinger, N.J., Bryant, R., & Shakesby, R.A. (2005). Effects of heating and post-heating equilibration times on soil water repellency. *Australian Journal of Soil Research, 43(3),* 261-267. doi:10.1071/sr04092

Doerr, S.H., Shakesby, R.A., & Walsh, R.P.D. (2000). Soil water repellency: its causes, characteristics and hydro-geomorphological significance. *Earth-Science Reviews, 51(1-4),* 33-65. doi:10.1016/S0012-8252(00)00011-8

Doerr, S.H., Shakesby, R.A., Dekker, L.W., & Ritsema, C.J. (2006). Occurrence, prediction and hydrological effects of water repellency amongst major soil and land-use types in a humid temperate climate. *European Journal of Soil Science, 57(5),* 741-754. doi:10.1111/j.1365-2389.2006.00818.x

Ekwue, E.I. (1990). Organic-matter effects on soil strength properties. *Soil and Tillage Research, 16(3),* 289-297. doi: 10.1016/0167-1987(90)90102-J

Emerson, W.W. (1967). A classification of soil aggregates based on their coherence in water. *Australian Journal of Soil Research, 5(1),* 47 – 57. doi:10.1071/SR9670047

Fattet, M., Fu, Y., Ghestem, M., Ma, W., Foulonneau, M., Nespoulous, J., &

Stokes, A. (2011). Effects of vegetation type on soil resistance to erosion: Relationship between aggregate stability and shear strength. *Catena, 87(1),* 60-69. doi:10.1016/j.catena.2011.05.006

Fuller, C. S. (1931). Oxidation of Solid Films of Tung Oil1 Mechanism of the Reaction at Elevated Temperatures. *Industrial & Engineering Chemistry, 23(12),* 1458-1462. doi:10.1021/ie50264a039

Goebel, M.O., Bachmann, J., Reichstein, M., Janssens, I.A., & Guggenberger, G. (2011). Soil water repellency and its implications for organic matter decomposition - Is there a link to extreme climatic events? *Global Change Biology, 17(8),* 2640-2656. doi:10.1111/j.1365-2486.2011.02414.x

Graber, E.R., Tagger, S., & Wallach, R. (2009). Role of divalent fatty acid salts in soil water repellency. *Soil Science Society of America Journal, 73(2),* 541-549. doi:10.2136/sssaj2008.0131

Hardin, B.O. (1985). Crushing of soil particles. *ASCE Journal of Geotechnical Engineering, 111(10),* 1177-1192. doi:10.1061/(ASCE)0733-9410(1985)111:10(1177)

Hong Kong 2018-19 Budget, (2018). 2018-19 Budget reports for the Hong Kong. https://www.budget.gov.hk/2018/eng/estimates.html (accessed 09 April 2019)

Jiménez-Pinilla, P., Doerr, S.H., Ahn, S., Lozano, E., Mataix-Solera, J., Jordán, A., Zavala, L.M., & Arcenegui, V., (2016). Effects of relative humidity on the water repellency of fire-affected soils. *Catena, 138,* 68-76. doi:10.1016/j.catena.2015.11.012

Kaiser, M., & Ellerbrock, R.H. (2005). Functional characterization of soil organic matter fractions different in solubility originating from a long-term field experiment. *Geoderma, 127(3-4),* 196-206. doi: 10.1016/j.geoderma.2004.12.002

Kořenková, L., & Matúš, P. (2015). Role of water repellency in aggregate

stability of cultivated soils under simulated raindrop impact. *Eurasian Soil Science, 48(7),* 754-758.

Laskowski, J., & Kitchener, J.A. (1969). The hydrophilic—hydrophobic transition on silica. *Journal of Colloid and Interface Science, 29(4),* 670–679. doi: 10.1016/0021-9797(69)90219-7

Letey, J., Carrillo, M.L.K., & Pang, X.P. (2000). Approaches to characterize the degree of water repellency. *Journal of Hydrology, 231-232,* 61-65. doi:10.1016/S0022-1694(00)00183-9

Li, M., & Zhang, H.Y. (2012). Hydrophobicity and carbonation treatment of earthen monuments in humid weather condition. *Science China - Technological Sciences, 55(8),* 2313-2320. doi:10.1007/s11431-012-4828-3

Lichner, L., Dlapa, P., Doerr, S.H., & Mataix-Solera, J. (2006). Evaluation of different clay minerals as additives for soil water repellency alleviation. *Applied Clay Science, 31(3-4),* 238-248. doi:10.1016/j.clay.2005.10.012

Liu, X.Y., Timar, M.C., Varodi, A.M. & Yi, S.L., (2015). Tung oil and linseed oil as traditional finishing materials important for furniture conservation. *PRO LIGNO,, 11(4)*, 571-579

Linker, R., Shmulevich, I., Kenny, A., & Shaviv, A. (2005). Soil identification and chemometrics for direct determination of nitrate in soils using FTIR-ATR mid-infrared spectroscopy. *Chemosphere, 61(5),* 652-658. doi: 10.1016/j.chemosphere.2005.03.034

Lourenço, S.D.N., Wakefield, C., Morley, C., Doerr, S.H., & Bryant, R. (2015). Wettability decay in an oil-contaminated waste-mineral mixture with dry-wet cycles. *Environmental Earth Sciences, 74(3),* 2563-2569.

Liu, D., & Lourenço, S.D.N. (2018). Time-dependency of soil water repellency induced by dimethyldichlorosilane. Proc., 7th International Conference on Unsaturated Soils, Hong Kong. (in press).

1 Ma'shum, M., Tate, M.E., Jones, G.P., & Oades, J.M. (1988). Extraction and
2 characterization of water-repellent materials from Australian soils. *Journal*
3 *of Soil Science, 39,* 99-110. doi:10.1111/j.1365-2389.1988.tb01198.x
4 Mainwaring, K., Hallin, I.L., Douglas, P., Doerr, S.H., & Morley, C.P. (2013).
5 The role of naturally occurring organic compounds in causing soil water
6 repellency. *European Journal of Soil Science, 64(5),* 667-680. doi:
7 10.1111/ejss.12078
8 Mataix-Solera, J., & Doerr, S.H. (2004). Hydrophobicity and aggregate stability
9 in calcareous top soils from fire-affected pine forests in southeastern
10 Spain. *Geoderma, 118(1-2),* 77-88. doi:10.1016/S0016-7061(03)00185-X
11 McKissock, I., Gilkes, R.J., Harper, R.J., & Carter, D.J. (1998). Relationships of
12 water repellency to soil properties for different spatial scales of study.
13 *Australian Journal of Soil Research, 36(3),* 495-507. doi: 10.1071/S97071
14 Mckissock, I., Gilkes, R.J., & Van Bronswijk, W. (2003). The relationship of soil
15 water repellency to aliphatic C and kaolin measured using DRIFT.
16 *Australian Journal of Soil Research, 41(2),* 251-265.
17 Ng, S.H.Y., & Lourenço, S.D.N. (2016). Conditions to induce water repellency
18 in soils with dimethyldicholorosilane, *Géotechnique, 66(5),* 441-444.
19 doi:10.1680/jgeot.15.T.025
20 Rabot, E., Wiesmeier, M., Schluter, S., & Vogel, H.-J., (2018). Soil structure as
21 an indicator of soil functions: A review. *Geoderma, 314,* 121-137.
22 doi:10.1016/j.geoderma.2017.11.009
23 Robichauda, P.R., & Hungerfordb, R.D. (2000). Water repellency by laboratory
24 burning of four northern Rocky Mountain forest soils. *Journal of Hydrology,*
25 *231-232,* 207-219. doi:10.1016/S0022-1694(00)00195-5
26 Saikia., B., & Parthasarathy, G. (2010). Fourier transform infrared
27 spectroscopic characterization of kaolinite from Assam and Meghalaya,
28 Northeastern India. *Journal of Modern Physics, 1(4),* 206-210. doi:

10.4236/jmp.2010.14031

Salama, W., El Aref, M., & Gaupp, R. (2015). Spectroscopic characterization of iron ores formed in different geological environments using FTIR, XPS, Mössbauer spectroscopy and thermoanalyses. *Spectrochim Acta A Mol Biomol Spectrosc,* 1816-1826. doi:10.1016/j.saa.2014.10.090

Samadzadeh, M., Boura, S.H., Peikari, M., Ashrafi, A., & Kasiriha, M. (2011). Tung oil: An autonomous repairing agent for self-healing epoxy coatings. *Progress in Organic Coatings, 70(4),* 383-387. doi: 10.1016/j.porgcoat.2010.08.017

Saulick, Y., Lourenço, S.D.N., & Baudet, J.P. (2017). A semi-automated technique for repeatable and reproducible contact angle measurements in granular materials using the Sessile Drop Method. *Soil Science Society of America Journal, 81(2),* 241-249. doi:10.2136/sssaj2016.04.0131

Savage, S.M., Osborn, J., Letey, J., & Heaton, C. (1972). Substances contributing to fire-induced water repellency in soils. *Soil Science Society of America Proceedings, 36,* 674-678. doi:10.2136/sssaj1972.03615995003600040047x

Schönemann, A., Kenndler, E., Frenzel, W. & Unger, Achim. (2006). An investigation of the fatty acid composition of new and aged tung oil. Studies in Conservation, Volume 51, p.99-110

Schönemann, A., & Edwards, H.G.M. (2011). Raman and FTIR microspectroscopic study of the alteration of Chinese tung oil and related drying oils during ageing. *Analytical & bioanalytical chemistry, 400(4),* 1173-1180. doi:10.1007/s00216-011-4855-0

Shogren, R.L., Petrović, Z., Liu, Z., & Erhan, S. (2004). Biodegradation behaviour of some vegetable oil-based polymers, *Journal of Polymers and the Environment, 12(3),* 173-178. doi:10.1023/B:JOOE.0000038549.73769.7d

Simkovic, I., Dlapa, P., Doerr, S. H., Mataix-Solera, J., & Sasinkova, V. (2008). Thermal destruction of soil water repellency and associated changes to soil organic matter as observed by FTIR spectroscopy. *Catena, 74(3),* 205-211. doi:10.1016/j.catena.2008.03.003

Subedi, S., Hamamoto, S., Komatsu, T., & Kawamoto, K. (2013). Development of hydrophobic capillary barriers for landfill covers system: Assessment of water repellency and hydraulic properties of water repellent soils. *Research Report of Department of Civil and Environmental Engineering,* Saitama University, Saitama, Japan, 39, 33-44.

Tang, X.W., Lin, T.S., Luo, X., Ying, F., & Li, Z. (2007). Strength and geoenvironmental properties of clay improved by tung oil and sticky rice juice. *Chinese journal of geotechnical engineering, 29(9),* 1324-1329.

Täumer, K., Stoffregen, H., & Wessolek, G. (2005). Determination of repellency distribution using soil organic matter and water content. *Geoderma, 125(1-2),* 107-115. doi:10.1016/j.geoderma.2004.07.004

Varela, M.E., Benito, E., & Keizer, J.J. (2015). Influence of wildfire severity on soil physical degradation in two pine forest stands of NW Spain. *Catena, 133,* 342-348. doi:10.1016/j.catena.2015.06.004

Wexler, H. (1964). Polymerization of drying oils. *Chemical Reviews, 64(6),* 591-611. doi:10.1021/cr60232a001

Yao, T. (2019). Characterization of soil grain surface roughness and its change with normal loading. PhD Thesis., The University of Hong Kong, Hong Kong SAR.

Zhang, H.Y., Zhu, S.B., Li, M., & Zhang, X.C. (2016). Water repellency of monument soil treated by tung oil. *Geotechnical and Geological Engineering, 34(1),* 205-216. doi:10.1007/s10706-015-9939-8

Zhao, P., Jackson, M.D., Zhang, Y.S., Li, G.Y., Monteiro, P.J.M., & Yang, L. (2015). Material characteristics of ancient Chinese lime binder and

experimental reproductions with organic admixtures. *Construction and Building Materials, 84,* 477-488. doi:10.1016/j.conbuildmat.2015.03.065

Zheng, S., Lourenço, S.D.N., Cleall, P., Chui, T.F.M., Ng, A., & Millis, S. (2017). Hydrologic behaviour of model slopes with synthetic water repellent soils, *Journal of Hydrology, 554,* 582-599. doi:10.1016/j.jhydrol.2017.09.013

Tables and figures

Table 1. Properties of Completely Decomposed Granite

Moisture content (%)	Soil organic matter content (%)	Specific gravity	Atterberg limits		Particle size distribution				Mineral Compound Concentration			
			Liquid limit	Plastic limit	Clay (%)	Silt (%)	Sand (%)	Gravel (%)	Quartz (%)	Kaolin (%)	Illite (%)	Gibbsite (%)
1.5-1.7	4.4-4.8	2.68	44	28	18	17	49	**16**	46	43	6	5

Table 2. Aggregate water stability (AS_{60}) and breakdown time (T_0) at different concentrations and heating conditions.

Heating Condition		Concentration (%)													
Temperature	Duration	0		1		2		5		8		10		15	
(°C)	(hour)	AS_{60}	T_0	AS_{60}	T_0	AS_{60}	T_0	AS_{60}	T_0	AS_{60}	T_0	AS_{60}	T_0	AS_{60}	T_0
25 (Control)	-	0%	0s	0%	0s	0%	5s	83%	-s	100%	-s	100%	-s	67%	1500 s
50	0.5	0%	0s	0%	5s	0%	10s	100%	-s	100%	-s	100%	-s	100%	-s
	5	0%	0s	0%	0s	0%	30s	100%	-s	100%	-s	100%	-s	100%	-s
150	0.5	0%	0s	0%	0s	0%	10s	100%	-s	83%	1800 s	100%	-s	100%	-s
	5	0%	0s	0%	5s	0%	60s	100%	-s	100%	-s	83%	2400 s	100%	-s
300	0.5	0%	0s	0%	10s	0%	10s	67%	1620 s	100%	-s	100%	-s	100%	-s
	5	0%	0s	0%	0s	0%	10s	100%	-s	100%	-s	100%	-s	100%	-s

Table 3. Gradient E_A at different heating conditions.

T	0.5-hour		1.0-hour		3.0-hour		5.0-hour	
(°C)	E_A	R^2	E_A	R^2	E_A	R^2	E_A	R^2
50	0.2621	0.9327	0.2698	0.9146	0.2773	0.9319	0.2822	0.9512
100	0.2602	0.9405	0.3093	0.8436	0.3107	0.9757	0.2945	0.8971
150	0.2647	0.7876	0.415	0.9778	0.4192	0.9463	0.3714	0.9256
200	0.7038	0.9619	0.5185	0.8431	0.4497	0.9473	0.6412	0.9205
250	0.7333	0.8347	0.6942	0.8338	0.7664	0.9702	0.4098	0.794
300	0.7371	0.773	0.9155	0.7796	0.9081	0.8622	0.4686	0.9567

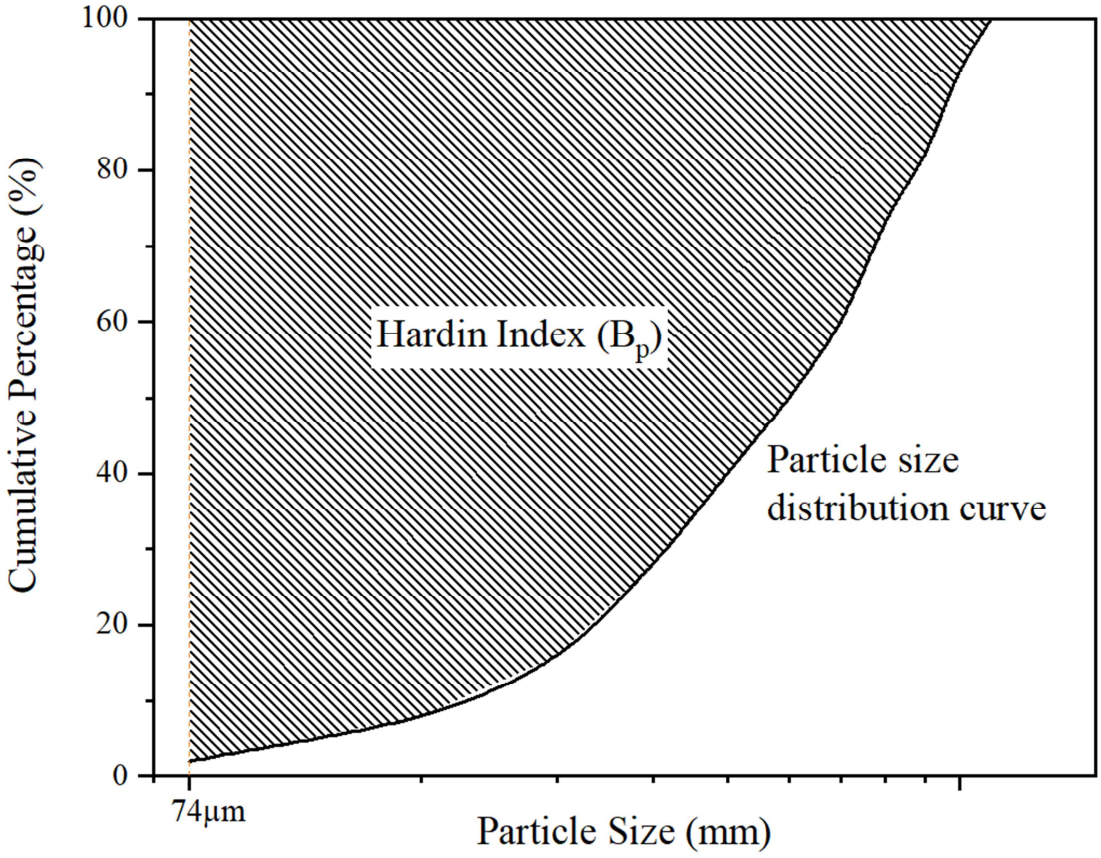

Figure 1. Hardin index (B_P).

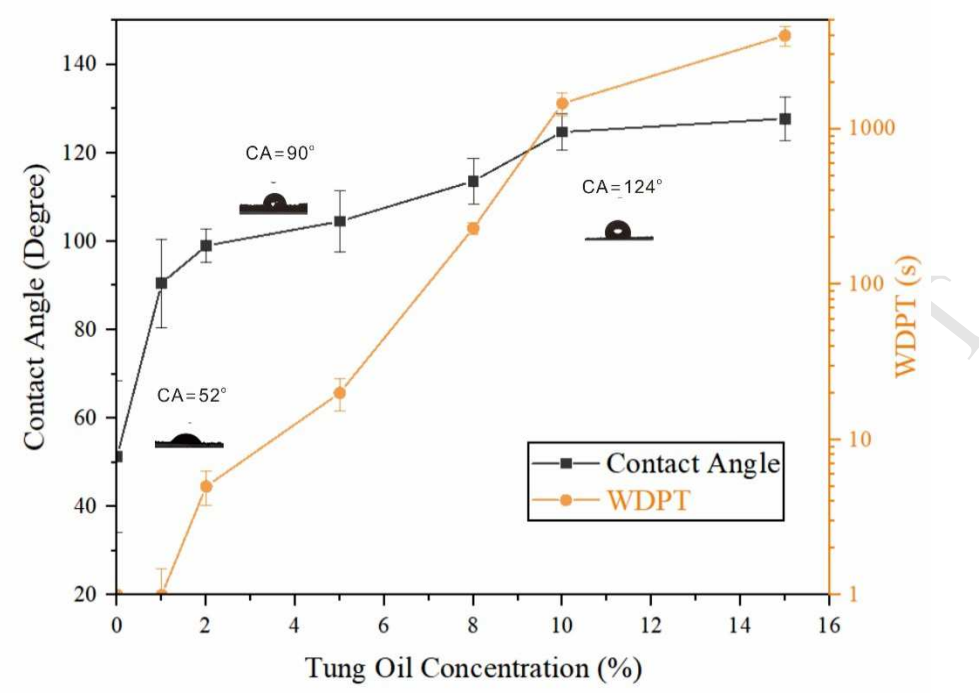

Figure 2. Contact angles and water drop penetration time for treated completely decomposed granite for different Tung oil concentrations.

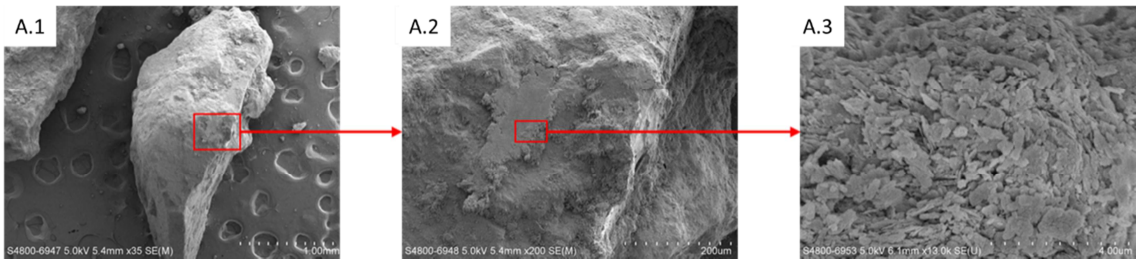

(a)

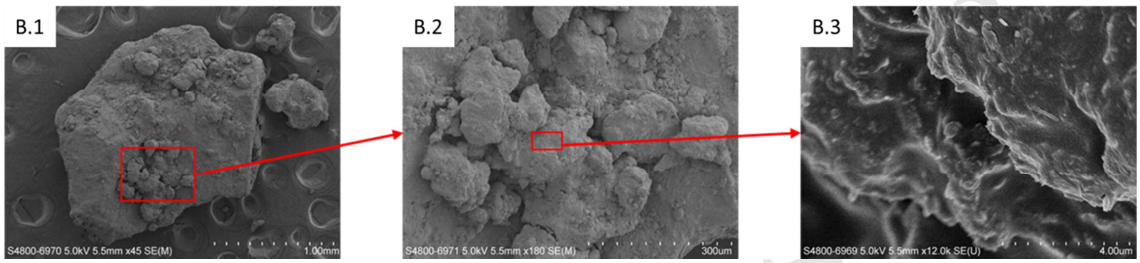

(b)

Figure 3. SEM images of (a) untreated and (b) treated completely decomposed granite (15% of concentration and unheated) at different scales (dashed bar), (A.1 and B.1) 1.00 mm, (A.2 and B.2) 300 µm, (A.3 and B.3) 4.00 µm.

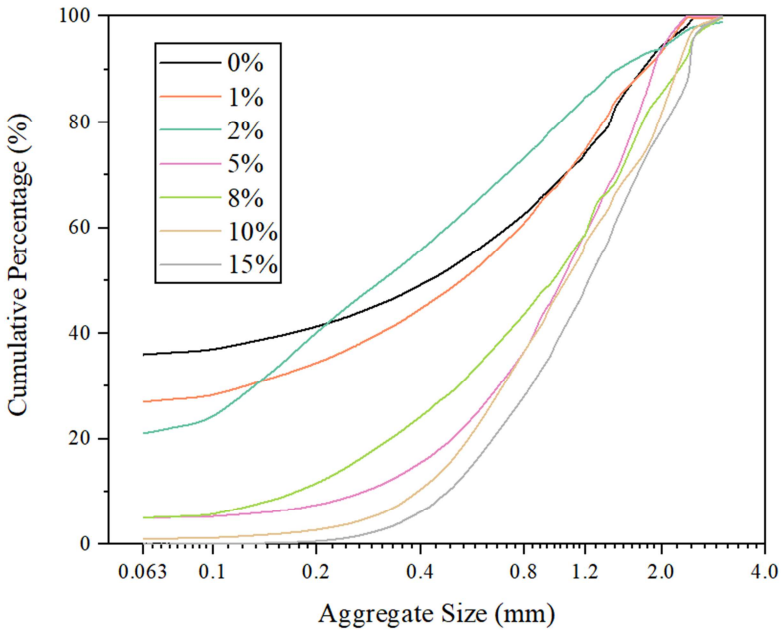

(a)

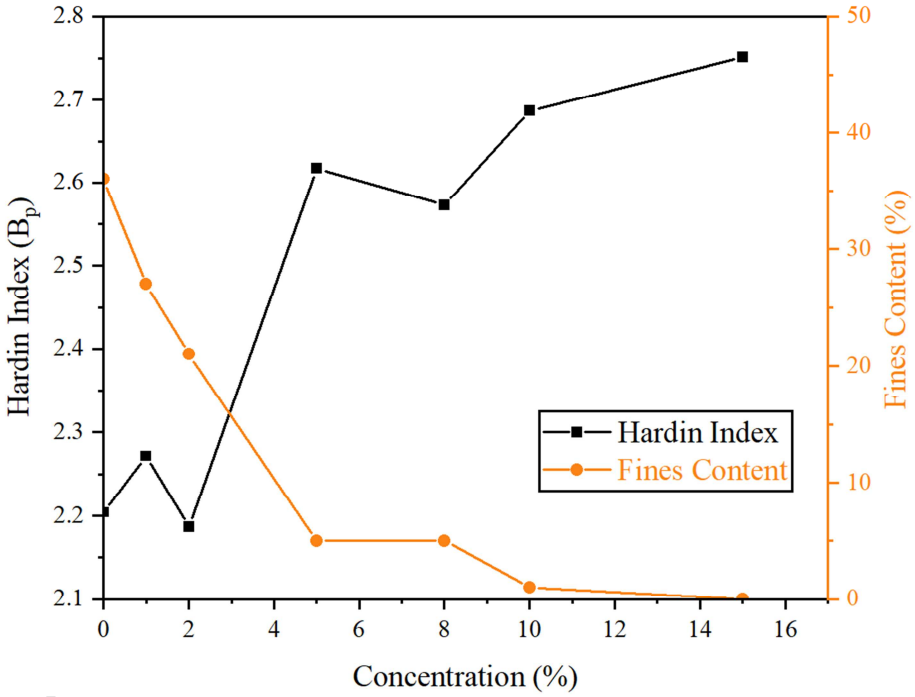

(b)

Figure 4. Soil aggregation at increasing Tung oil concentrations (unheated) represented by (a) Aggregate Size Distribution; and (b) Hardin index and fines content.

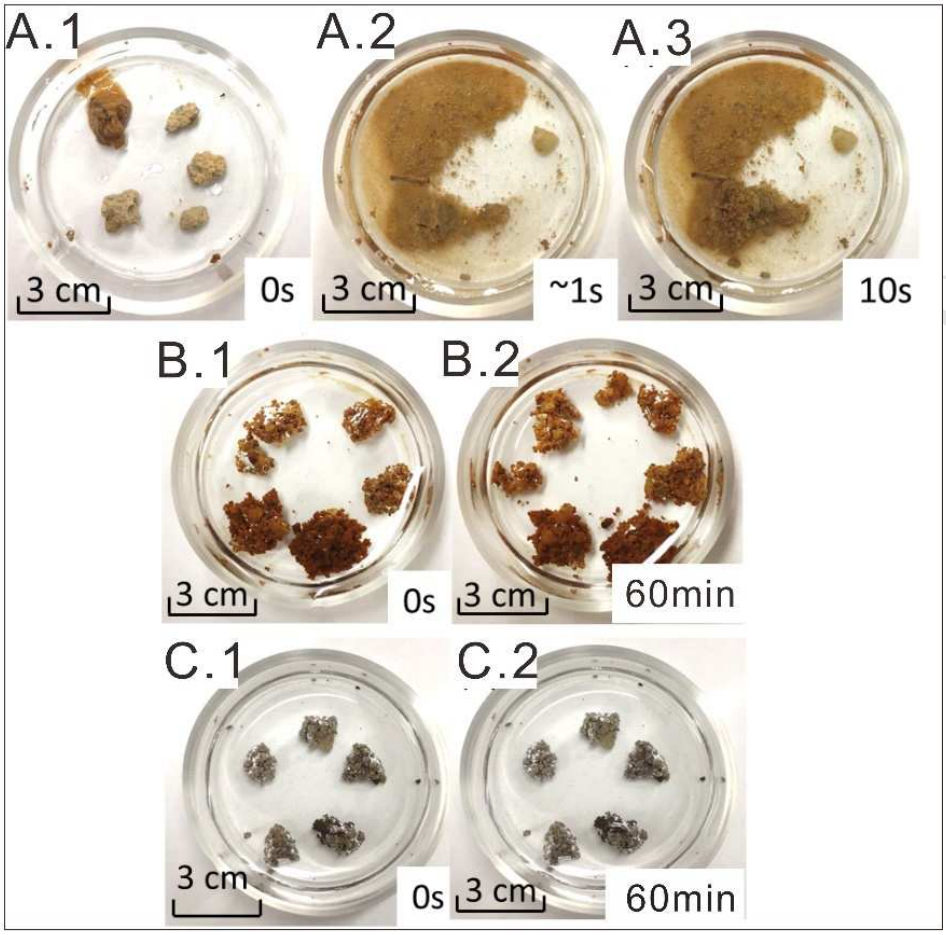

Figure 5. Water immersion behaviour of completely decomposed granite (a) untreated, (b) treated aggregates (15%) before heating and (c) treated aggregates after heating (15%, and 300°C for 5 hours).

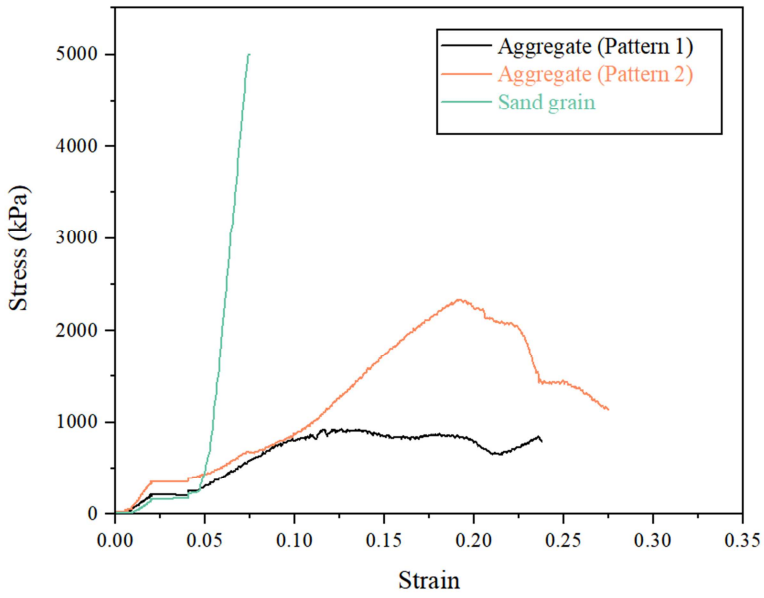

(a)

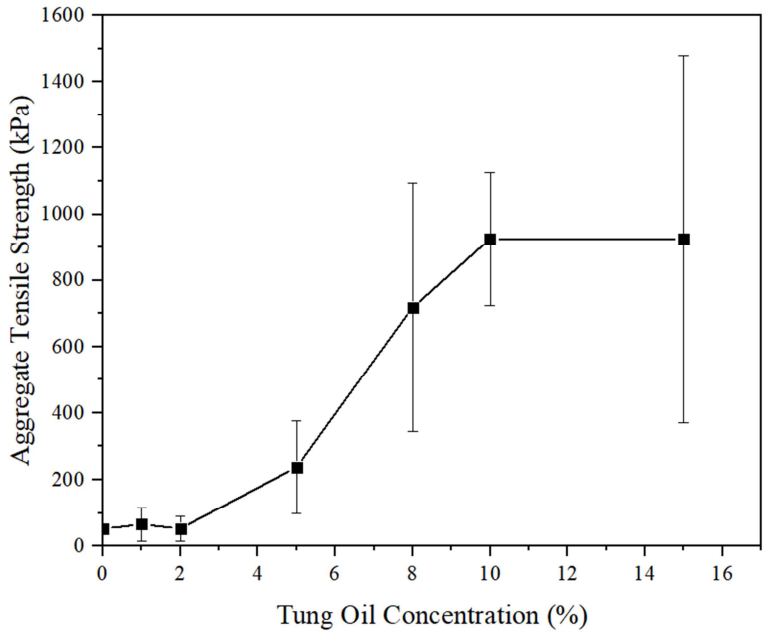

(b)

Figure 6. Aggregate tensile strength of treated completely decomposed granite (unheated) (a) stress-strain curves of aggregates with 15% Tung oil concentration and a sand grain (pattern 1 = softer aggregate; pattern 2 = stiffer aggregate; and (b) concentration effect (error bar stands for standard deviation).

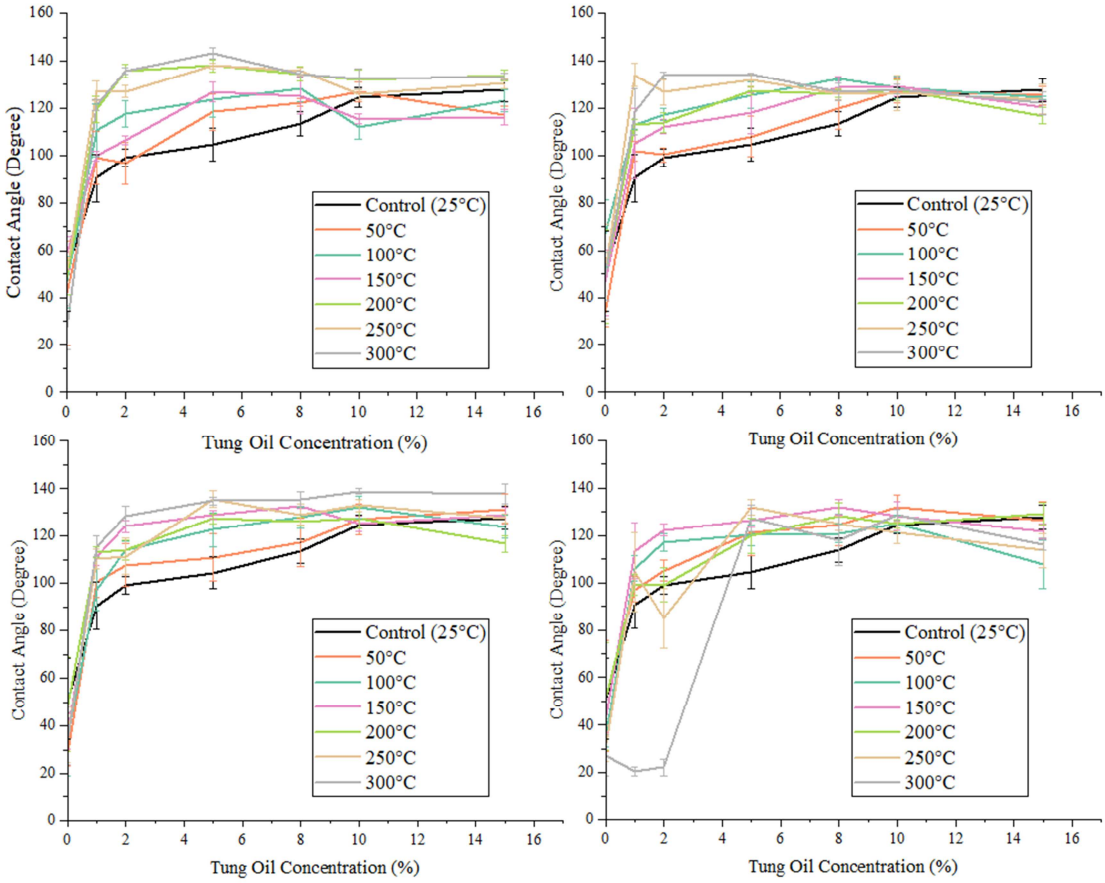

Figure 7. Contact angles of treated completely decomposed granite for different heating durations (a) 0.5-hour, (b) 1.0-hour, (c) 3.0-hour and (d) 5.0-hour durations.

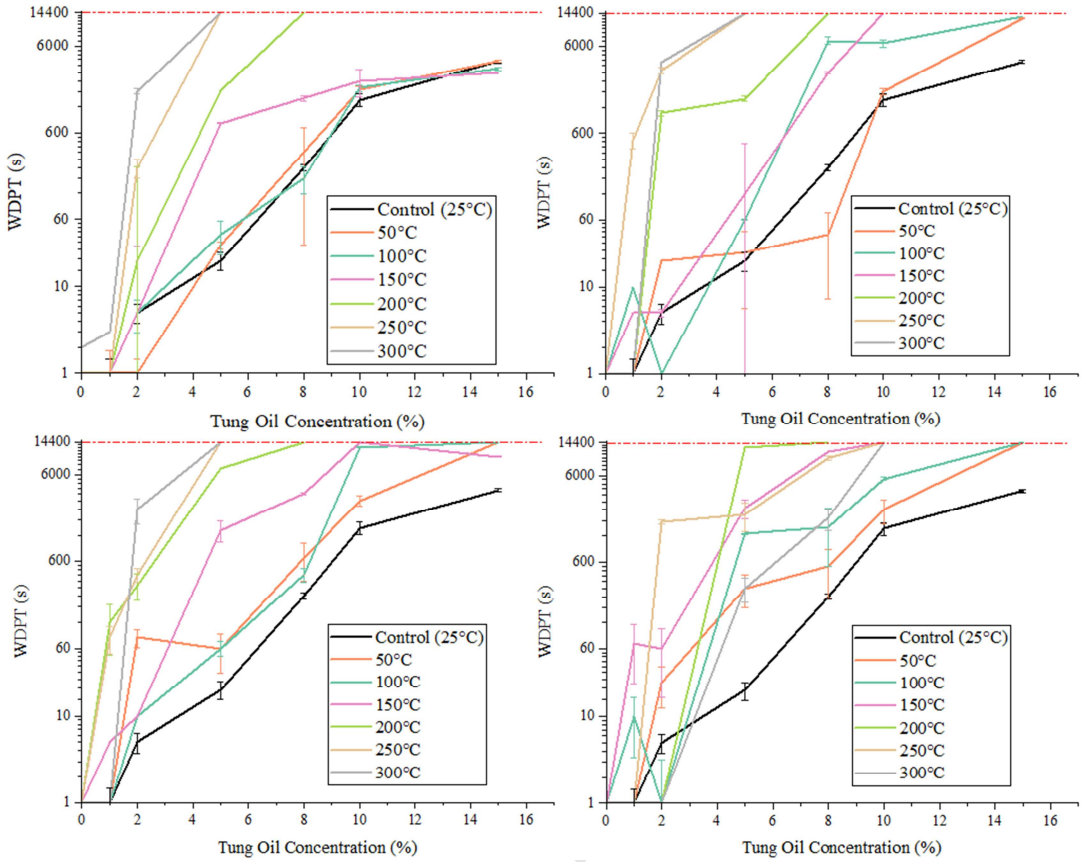

Figure 8. Water Drop Penetration Time of treated completely decomposed granite for different heating durations, (a) 0.5-hour, (b) 1.0-hour, (c) 3.0-hour and (d) 5.0-hour; dashed line refers to the upper measurement limit (14400s).

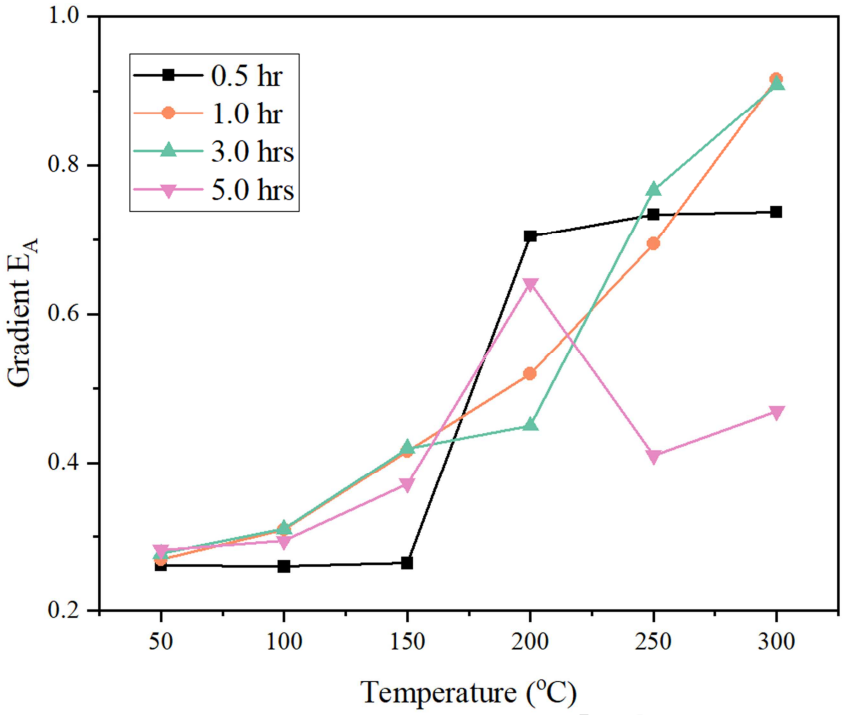

Figure 9. Gradient E_A for different heating durations.

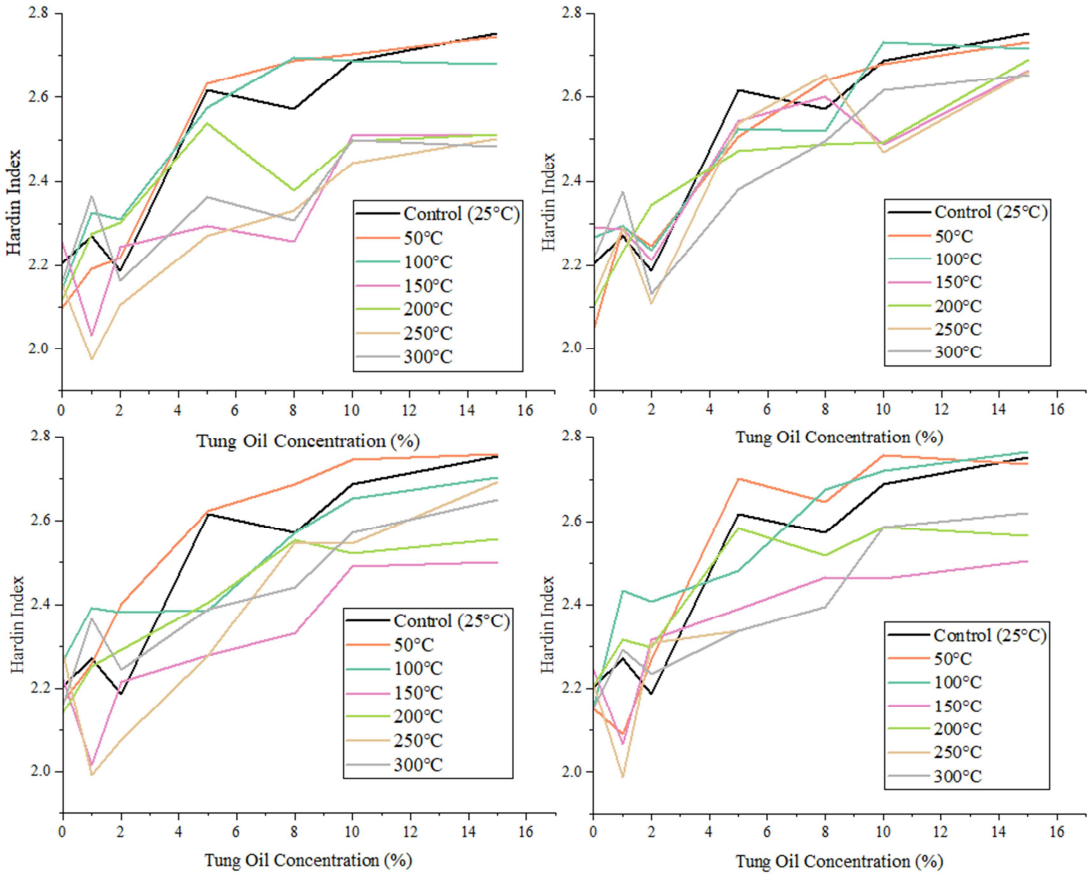

Figure 10. Hardin index of treated completely decomposed granite for different heating durations (a) 0.5-hour, (b) 1.0-hour, (c) 3.0-hour and (d) 5.0-hour durations.

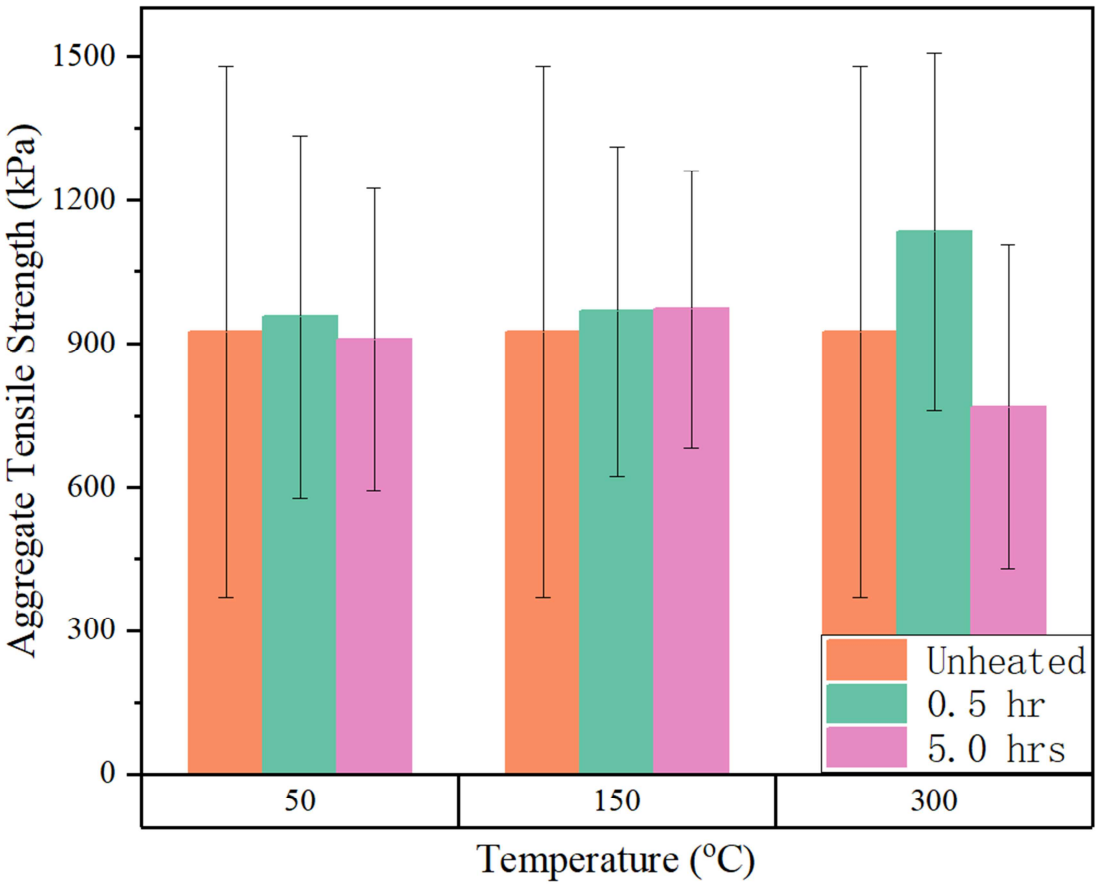

Figure 11. Aggregate tensile strength of treated completely decomposed granite at different heating conditions.

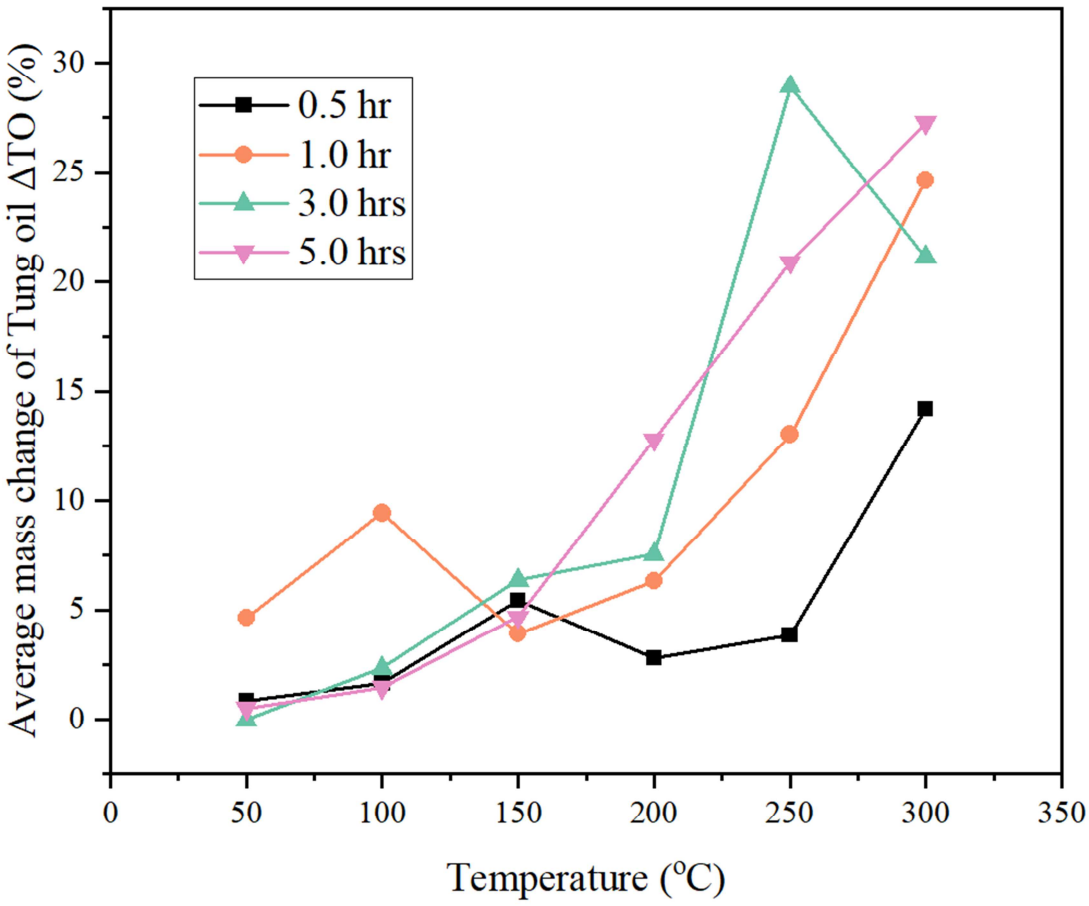

Figure 12. Average loss of Tung oil of treated completely decomposed granite with 1 - 15% of concentrations for different heating conditions.

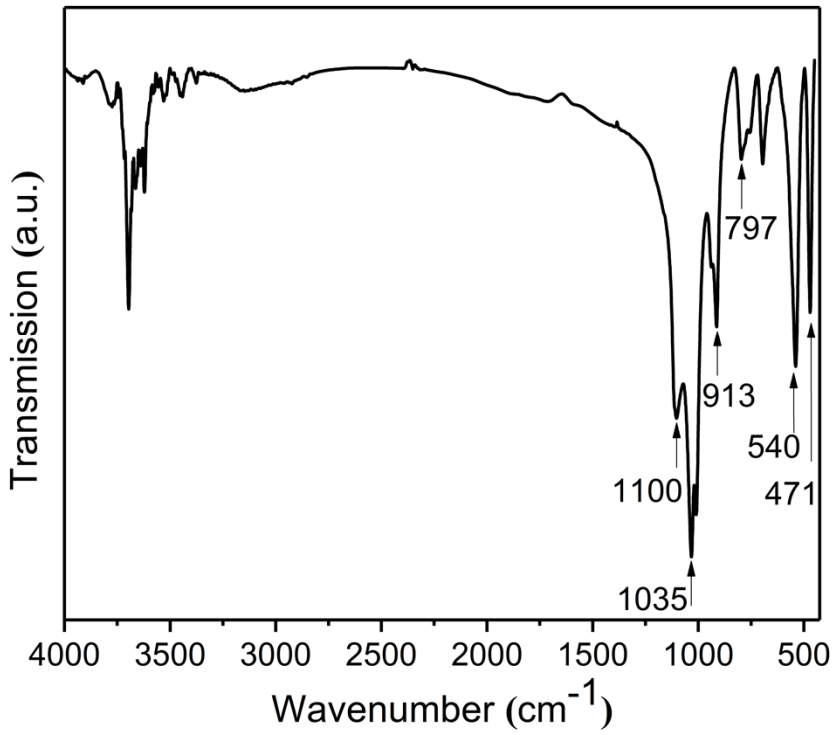
Transmission (a.u.)
797
913
540
1100
471
1035
4000
3500
3000
2500
2000
1500
1000
500
Wavenumber (cm-1)

(a)

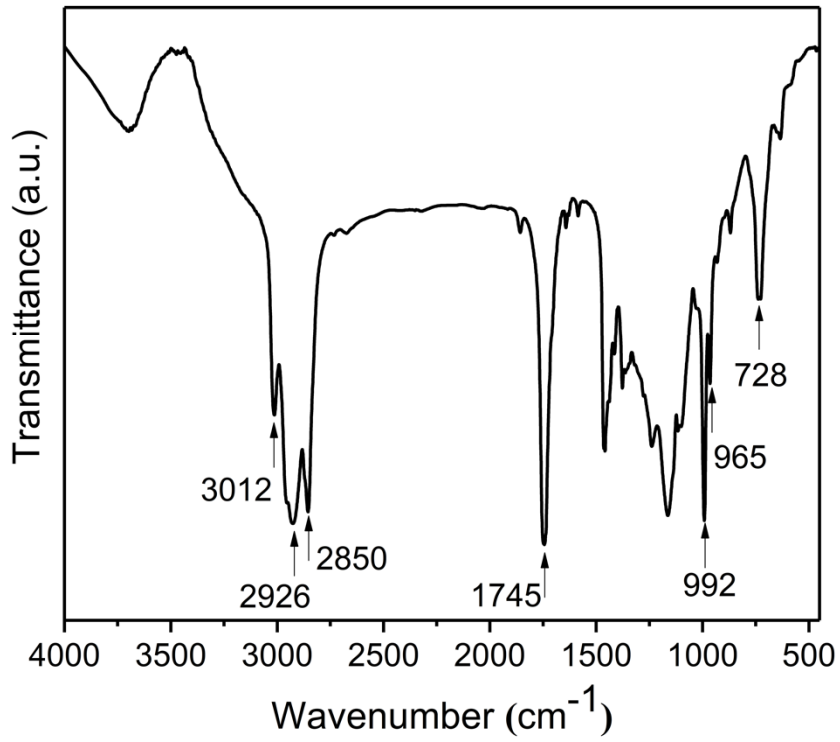
Transmittance (a.u.)
728
965
3012
2850
2926
1745
992
4000
3500
3000
2500
2000
1500
1000
500
Wavenumber (cm-1)

(b)

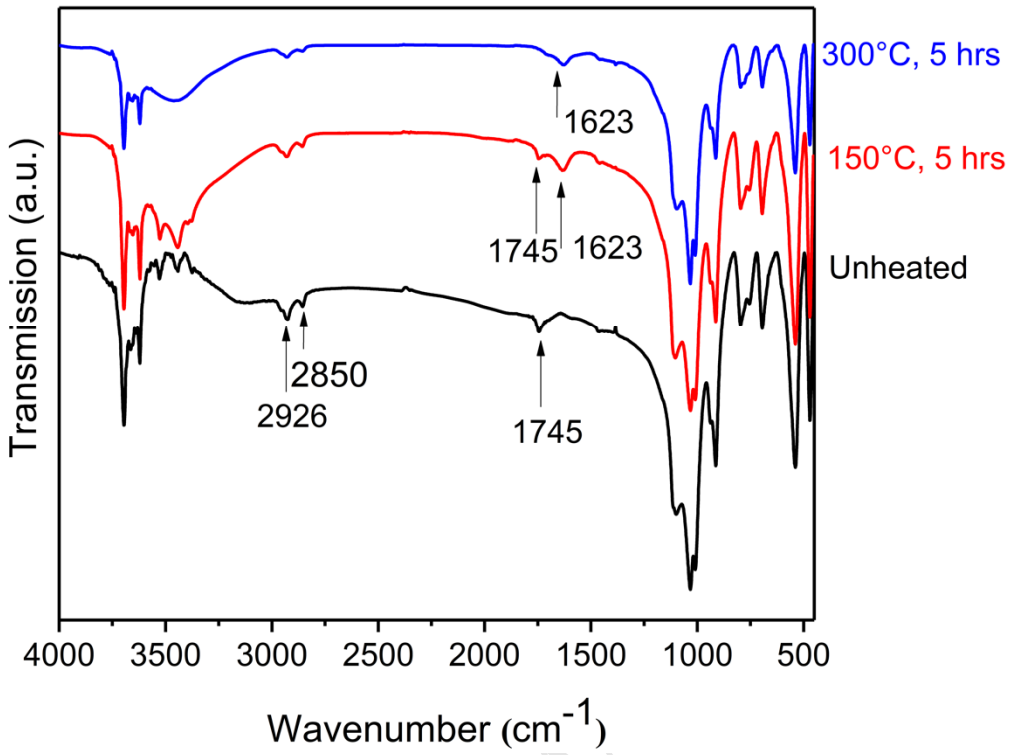

(c)

Figure 13. FTIR spectra for (a) completely decomposed granite, (b) Tung oil, (c) treated completely decomposed granite with 5% Tung oil.

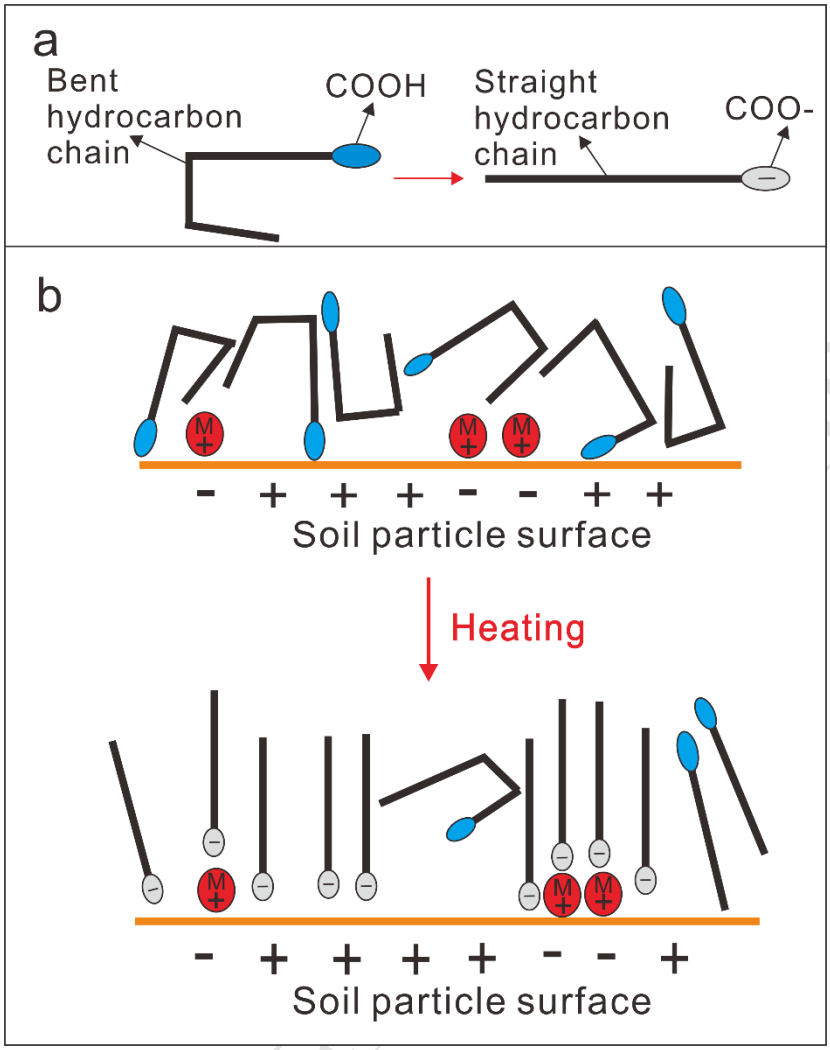

Figure 14. Molecular rearrangements at the particle surface (a) cis-trans isomerization and conversion of COOH to COO^- and (b) orientation change of molecules on the particle surface.

Supplementary Information

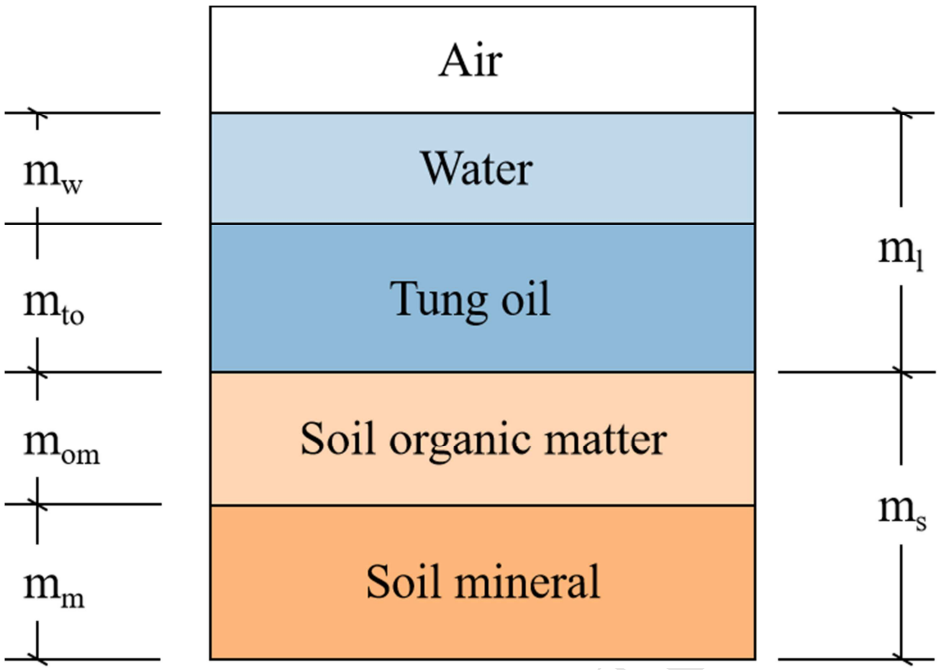

Figure 1. Idealized representation of Tung oil-treated completely decomposed granite in three phases: air, liquid (Tung oil and water) and solid (soil organic matter and soil mineral).